

FINAL REPORT

(NASA-CR-176481) FATIGUE BEHAVIOR OF
FLEXHOSES AND BELLOWS DUE TO FLOW-INDUCED
VIBRATIONS Final Report, 11 Jan. 1985 -
10 Jan. 1986 (Georgia Inst. of Tech.) 84 p
IC A05/MF A01

N86-19662

Unclas

CSCS 20K G3/39 05506

FATIGUE BEHAVIOR OF FLEXHOSES AND BELLOWS DUE TO FLOW-INDUCED VIBRATIONS

Prepared by

Prateen V. Desai
Principal Investigator
and
Lindsey Thornhill
Graduate Research Assistant



Prepared for

NASA Kennedy Space Center

Under

Contract No. NAG10-0017

January 1986

GEORGIA INSTITUTE OF TECHNOLOGY

A UNIT OF THE UNIVERSITY SYSTEM OF GEORGIA
SCHOOL OF MECHANICAL ENGINEERING
ATLANTA, GEORGIA 30332



FINAL REPORT

on

FATIGUE BEHAVIOR OF FLEXHOSES & BELLOWS DUE TO FLOW-INDUCED VIBRATIONS

Sponsor:

NASA Kennedy Space Center

Sponsor Contract No: NAG10-0017

Prepared by

Prateen V. Desai
Principal Investigator

and

Lindsey Thornhill
Graduate Research Assistant

George W. Woodruff School of Mechanical Engineering
Georgia Institute of Technology

January 1986

ABSTRACT

This report summarizes the analysis and results developed in a fresh approach to calculate flow induced vibration response of a flexible flow passage. The vibration results are further examined in the frequency domain to obtain dominant frequency information. A cumulative damage analysis due to cyclic strains is performed to obtain number of cycles to failure for metallic bellows of particular specifications under a variety of operational conditions. Sample plots of time and frequency domain responses are included in Appendix I. Complete listing of a computer program is provided in this report as Appendix II. The program successively executes each of the analyses needed to calculate the vibration response, the frequency response, the cyclic strains and the number of cycles to failure. The program prompts the user for necessary input information. Sample data from the program is provided in Appendix III. The fatigue life results obtained by the computer model lie within an acceptable range of previously measured available data.

I. INTRODUCTION

Project Background and Overview

This report describes all the work performed by Georgia Institute of Technology, College of Engineering, School of Mechanical Engineering under Grant number NAG10-0017, "Fatigue Behavior of Flexhoses & Bellows Due to Flow Induced Vibrations". This study was performed for the Kennedy Space Center of the National Aeronautics and Space Administration.

The general objective of this work was to investigate the physical phenomena associated with flow-induced vibrations of a flexible line in order to develop a methodology to examine its fatigue life. In response to NASA needs, much emphasis was placed on developing a computational procedure for calculating the number of cycles to failure for a specific bellows based on the assumed vibration model.

Flexible expansion joints are currently being used in a variety of applications. These include the nuclear reactor cooling systems, supply and return loading lines for submarines from the mother ship on the base, liquid cryogenic fuel lines for the space shuttle external tanks and so forth. There is, in fact, a manufacturer's association for expansion joints which publishes its recommended practices for their use.

Serious difficulties are encountered when practical solutions are not obtained to control the so-called "self-generated" sound or vibrations in flow systems which use such corrugated lines. For the special case of the internally corrugated flexible hoses, segments of which are utilized in the feed lines of Space Shuttle external tanks, a qualitative mechanism was identified in terms of the fluid flow related parameters governing the physical phenomena [1]. Unshrouded hose vibration was attributed to an approximate matching between the longitudinal structural frequency and the

frequency of vortex shedding at a critical flow velocity over the first few corrugations in the hose. This led to the computation of the modal frequencies of vibration by representing the hose with a series of lumped spring-mass elements and relating the amplitude of vibrations to the damping characteristics of the system. It was found necessary to supplement the postulated model by a large number of empirical correlations obtained from a series of experiments to relate the system geometry, the mean flow rate and the fluid properties with the modal frequencies and amplitudes of vibration, the damping characteristics, the maximum alternating stress and the expected fatigue life of the hose material [2].

Experimental observations under simulated field conditions have proved the predicted failure results of the two cited works to be very conservative. Furthermore, an overwhelming reliance on empirically obtained functions to predict the fatigue life of the hose in these studies has made it cumbersome to directly utilize the suggested failure prediction procedure. Flex line flow-induced vibrations were also examined in another study [3] with an eye to developing a methodology to assess its fatigue life. The cavity resonance model utilized in this work tends to be extra sensitive to minor parameter variations in predicting the time to failure by fatigue stresses. It appears that a definite need exists in developing a vibrational model for the flexible line that incorporates the interactive dynamics between fluid flow past cavities and the flow-induced vibration of the convolutes of the bellows configuration.

In the context of flow past cavities, there are three types of self generated oscillations. These are the fluid-dynamic, the fluid-resonant and the fluid elastic types of oscillations [4,5]. The fluid dynamic oscillations arise from some type of flow instability inherent to the flow configuration.

The fluid-resonant oscillations occur due to standing wave resonance effects which are particularly important for compressible fluid flow. The fluid-elastic oscillations involve a coupling of the solid boundary vibrations with the fluid flow perturbations causing those. It is this coupling which must be quantitatively included in the vibration model which predicts the convolute deformations. Subsequent cyclic strain analysis and the fatigue damage due to it are also examined in this work.

Statement of Research Problem

This research concerns the development of a vibration model as well as fatigue damage analysis to estimate life cycles of a bellows or a flexhose with a single- or multiply wall construction. The vibration model emphasises the coupled interactive nature of the fluid flow and structural vibrations. The vibration response is further examined to assess the dominant frequencies causing fatigue damage. Finally, the research adopts existing theories of cumulative fatigue damage with the results of vibration analysis to assess the number of cycles to failure of the bellows.

Flow Past Cavities

One of the first modifications to improve currently existing models of flow excitation in a bellows geometry concerns the force acting on each individual convolute. A preponderance of previously published information concerns flow past rectangular cavities. Of particular interest is the pressure distribution along the walls of the cavity.

Sketches of flow patterns in a rectangular cavity based on photographs [6] are shown in Figures 1(a), (b) and (c).

A plot of the measured pressure distribution [6] along the cavity wall for three different values of aspect ratio, h/b (0.5, 2.0, 1.5) reveals a trend shown in Figure 2. Similar plot [7] is shown in Figure 3. On the other

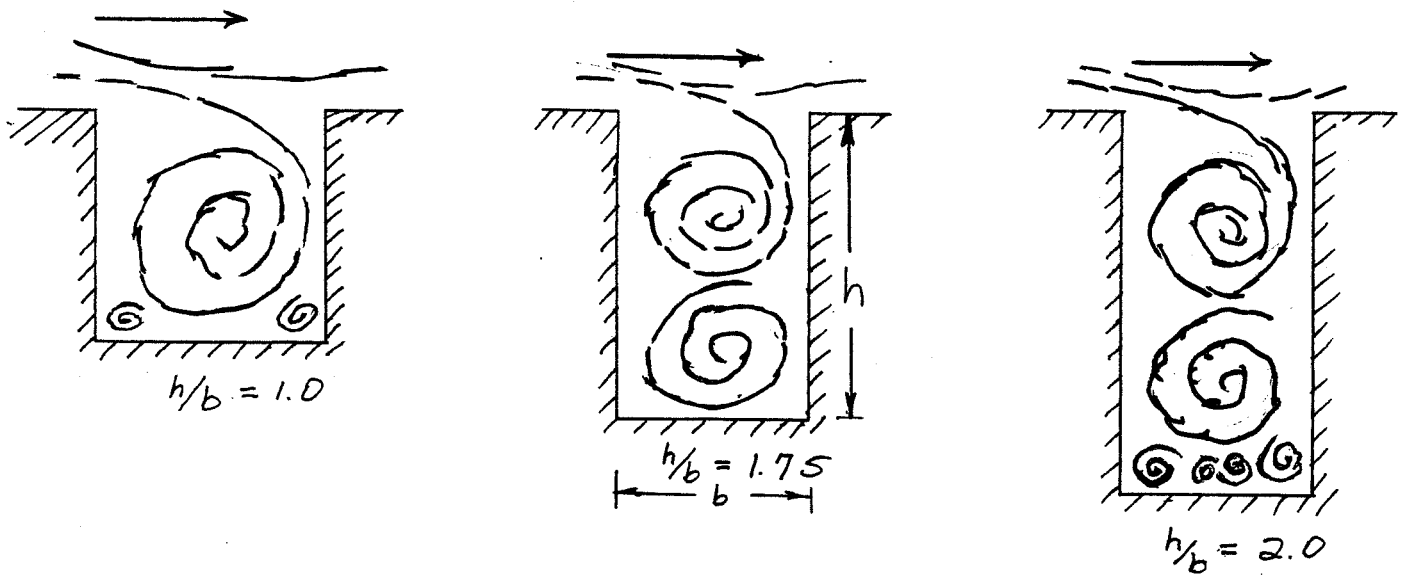


Figure 1. Sketches of Flow Past Square Cavities Based on Photography [6].

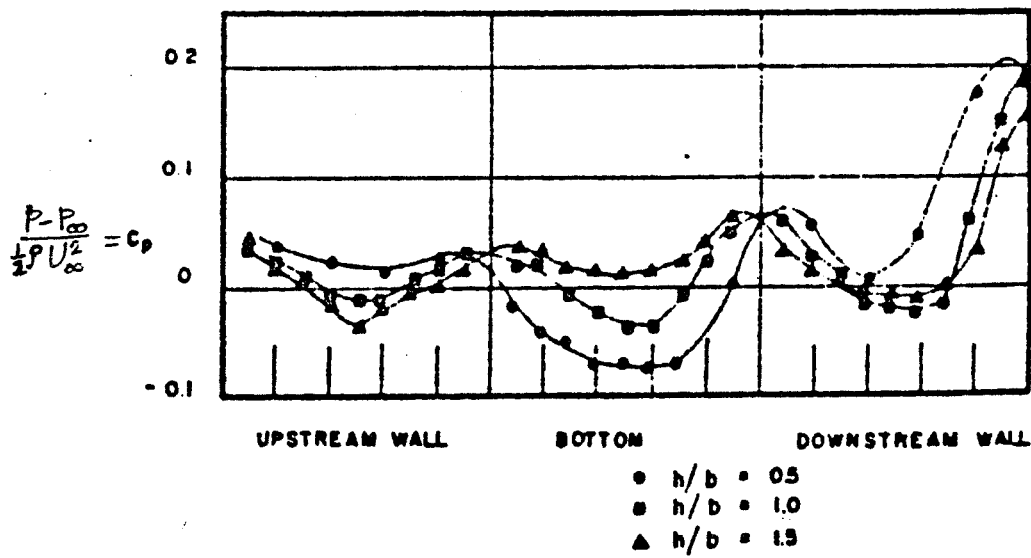


Figure 2. Typical Measured Pressure Distributions Along Cavity Wall Showing Influence of Height-to-width Ratio [6].

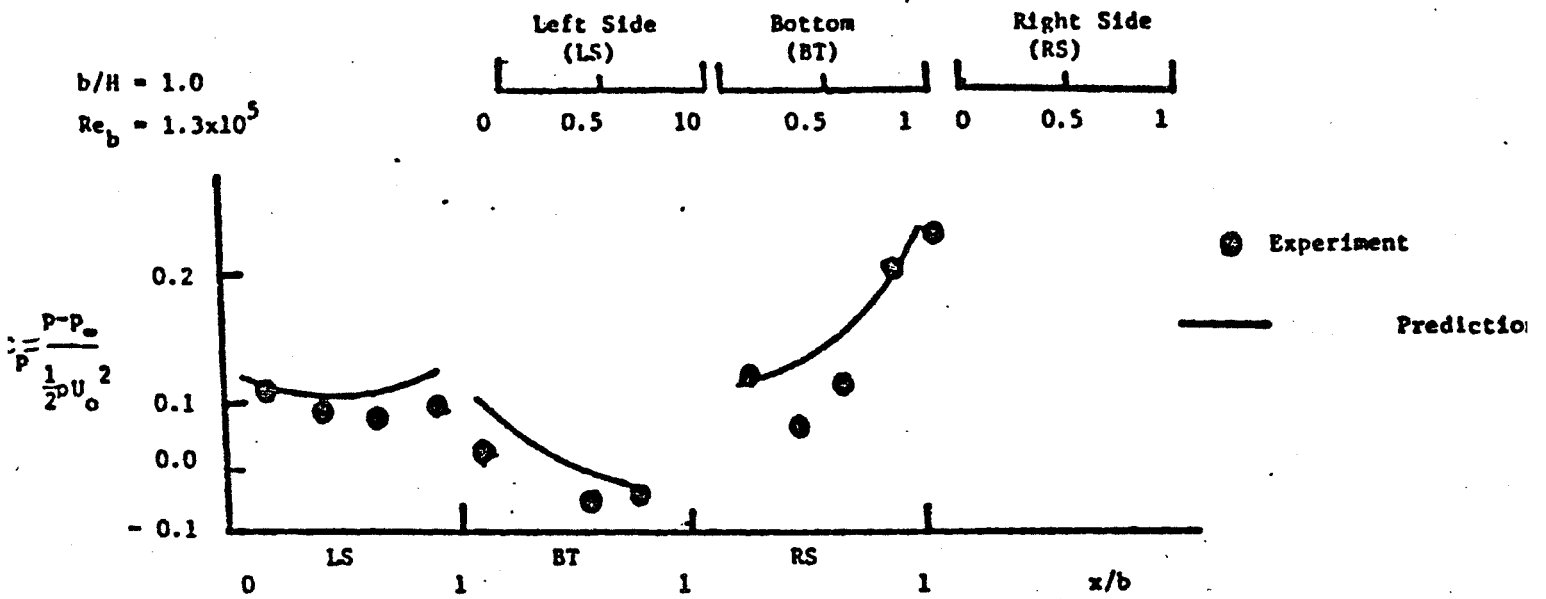
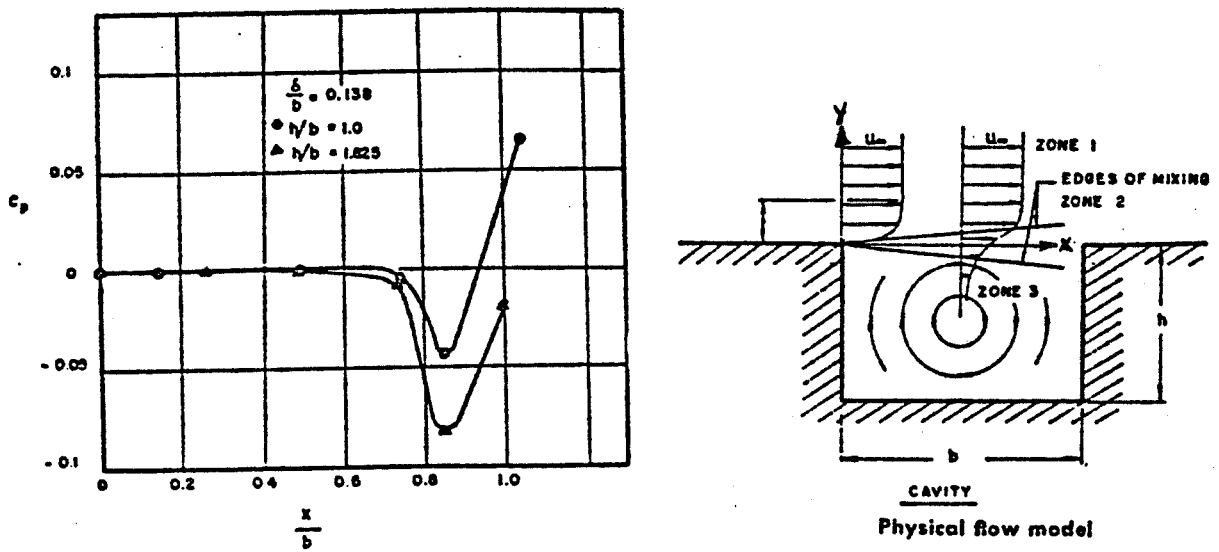


Figure 3. Pressure Distribution Along Square Cavity Walls [7].



Typical longitudinal pressure distribution in shear layer
 $y = 0$

Figure 4. Pressure Distribution From Analytical Model [6].

hand, an analytical model and its results of pressure variation along horizontal axis [6] are shown in Figure 4. It is seen that there is a pressure maximum at an area of flow reattachment on the downstream wall of the cavity.

On the assumption that these same trends hold for flow past a convolute-shaped cavity, the expected flow patterns are as shown in Figure 5. The maximum wall pressure is shown acting near the top of the downstream wall as demonstrated in the earlier results on cavity flow. The drop in pressure just previous to the sharp pressure rise shown in the plots might be explained by the vortices in the recirculating flow on the downstream wall. The vibrations of the bellows cause these recirculating vortices to move along the wall and be shed from the convolute tip periodically. As a vortex crosses the region of maximum pressure it causes a drop in this pressure. After the vortex has been shed the maximum pressure is reestablished, thus producing a fluctuating force. This fluctuating pressure force, along with an acoustical resonance (radial) that may exist, could produce relatively high pressure levels resulting in a bending of the convolute.

The maximum pressure force pictured may be broken down into transverse and axial components. Previous research has described the force acting on the convolute as a longitudinal force. Actually, this longitudinal force is seen in the present research as only the horizontal component of the maximum pressure force.

II. DEVELOPMENT OF THE MATHEMATICAL MODEL

Assessment of fatigue failure of metallic bellows due to flow induced vibrations requires

- a. the development of a coupled fluid-structure interactive vibration

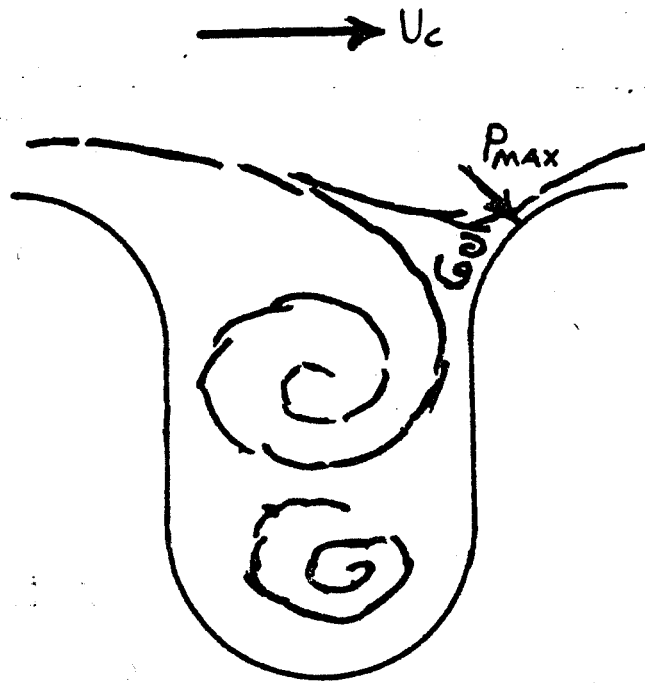


Figure 5. Impact Pressure Due to Flow Past a Convoluted Cavity.

- model to predict individual convolute deformations,
- b. a frequency domain analysis of the vibrational response to identify dominant frequencies causing the damage
- and
- c. a failure analysis based on available cumulative damage theories to calculate the number of cycles to failure.

Flow Induced Vibration Model

The interactive dynamics of bellows vibrations due to fluid flow over a cascade of convoluted cavities, which in turn modifies the fluid flow and forces that excite the vibrations, is a coupled nonlinear phenomena. It is governed by fluid flow conditions, the bellows geometry and the material response behavior.

The effective excitation force is internally generated and an analysis must be performed to express it in terms of identifiable physical quantities. The vibration of an individual convolute within a multiconvolute bellows in response to the excitation may be examined via lumped springs and masses in terms of physical quantities.

The Excitation Force

A comprehensive analysis of flow induced vibration of a bellows must consider the motion of an individual convolute in two coordinate directions. These directions correspond to the longitudinal and the transverse motion of the convolute as illustrated in Figure 6(a).

An expression for the excitation force acting on the convolute must account for the variation of the force due to convolute motion. When the bellows are absolutely motionless the flow geometry is that illustrated in Figure 6(b). This flow may be represented by the velocity triangle in Figure 7(a).

In this figure, α_0 , estimated from data on flow past cylinders [8], is

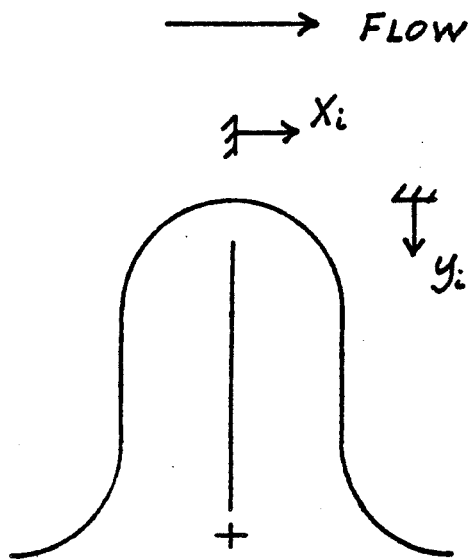


Figure 6a. Coordinate System to Analyze Convolute Deformation.

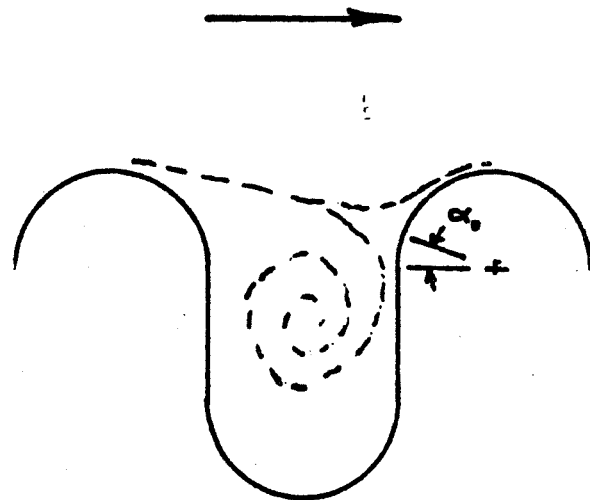


Figure 6b. Configuration for Undeformed Bellows.

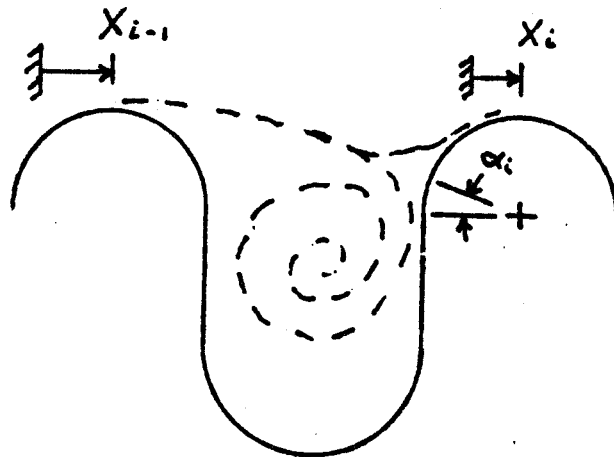


Figure 6c. Convolute Deformation Along x.

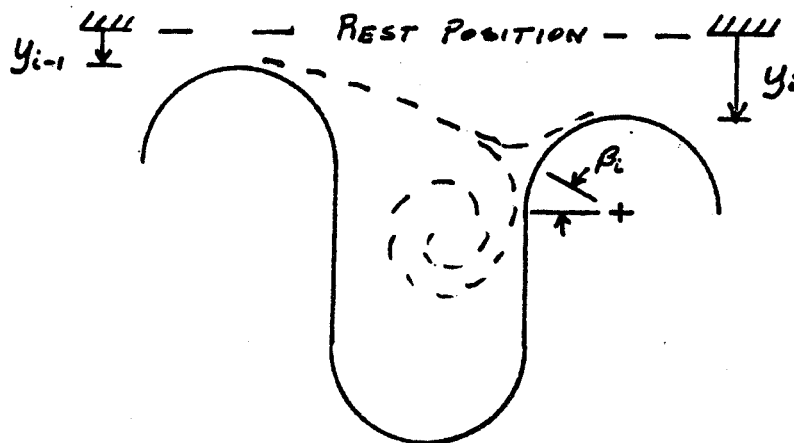


Figure 6d. Convolute Deformation Along y.

the angle between the velocity of the flow approaching the convolute tip, U_0 , and the velocity of the core flow, U_c . The flow configuration illustrated in Figure 6(b) produces force coefficients on the convolute tip given by

$$C_{o,x} = \frac{U_0^2}{U_c^2} (C_D \cos \alpha_0 + C_L \sin \alpha_0) \quad (1a)$$

and

$$C_{o,y} = \frac{U_0^2}{U_c^2} (C_D \sin \alpha_0 + C_L \cos \alpha_0) , \quad (1b)$$

where C_D and C_L are drag and lift coefficients, respectively, of convolute tip in the core flow; C_D and C_L are estimated from flow past cylinders [8].

When the convolute tip is displaced longitudinally, the configuration illustrated in Figure 6(c) results. The angle made by the flow approaching the convolute tip with the core velocity, $\alpha_i (= \alpha_0 + \Delta\alpha)$ is shown on the velocity triangle in Figure 7(b) representing this situation. In this figure, $U_{r,x,i}$ is the velocity of the flow approaching the i^{th} convolute tip relative to the convolute longitudinal velocity. The force coefficients for this situation become

$$C_{x,i} = \frac{U_{r,x,i}^2}{U_c^2} (C_D \cos \alpha_i + C_L \sin \alpha_i) \quad (2a)$$

and

$$C_{y,i} = \frac{U_{r,x,i}^2}{U_c^2} (C_D \sin \alpha_i + C_L \cos \alpha_i) . \quad (2b)$$

These expressions show that longitudinal motion of the convolute produces a variation in both the longitudinal and transverse excitation forces. Therefore, longitudinal motion cannot exist independent of transverse motion.

When the convolute tip is displaced in the transverse direction, the

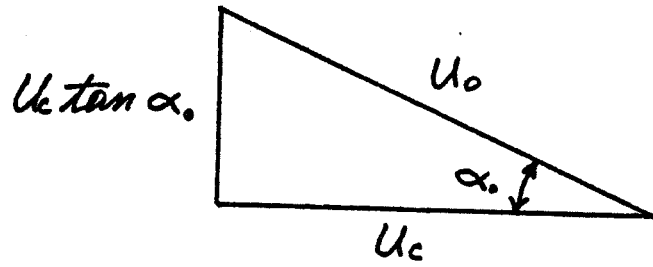


Figure 7a. Velocity Triangle: Un-deformed Bellows.

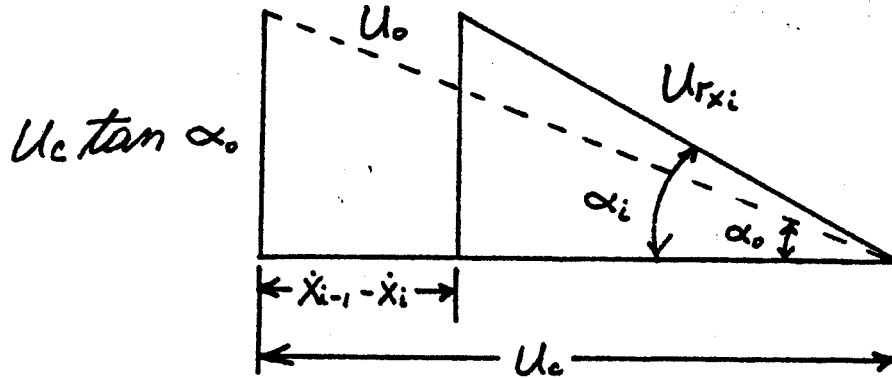


Figure 7b. Velocity Triangle: Deformation Along x.

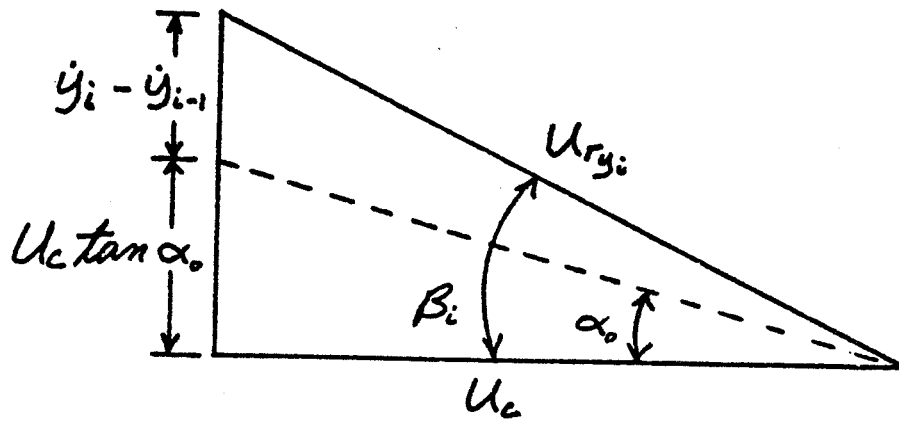


Figure 7c. Velocity Triangle: Deformation Along y.

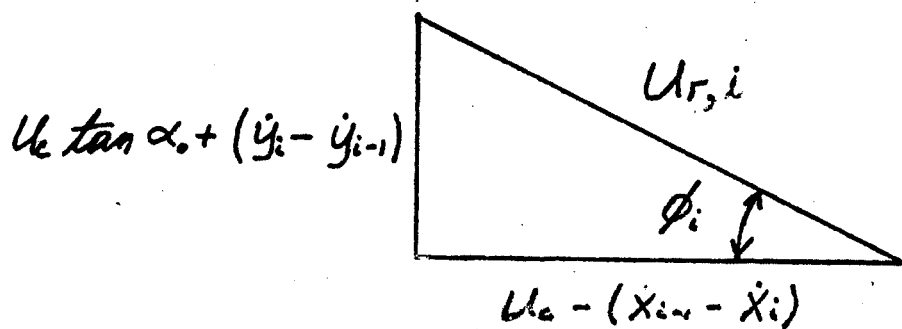


Figure 8. Velocity Triangle Combined x & y Deformation.

configuration shown in Figure 6(d) represents the situation. The new angle, β_i , made by the approaching flow with the core velocity ($\beta_i = \alpha_0 + \Delta\beta$) is shown on the velocity triangle in Figure 7(c). In this figure $U_{r,y,i}$ is the velocity of the flow approaching the i^{th} convolute tip relative to the convolute transverse velocity. The force coefficients for this variation are

$$C_{x,i} = \frac{U_{r,y,i}^2}{U_c^2} (C_L \sin\beta_i + C_D \cos\beta_i) \quad (3a)$$

and

$$C_{y,i} = \frac{U_{r,y,i}^2}{U_c^2} (C_L \cos\beta_i + C_D \sin\beta_i) . \quad (3b)$$

Similar to the case for longitudinal motion, transverse motion causes variation in both the longitudinal and transverse forces acting on the convolute tip. Therefore, transverse motion cannot exist independent of longitudinal motion.

If the transverse and longitudinal displacements are allowed to occur simultaneously, the velocity triangle becomes that shown in Figure 8. From this figure the angle ϕ_i and the relative velocity $U_{r,i}$ may, respectively, be determined as

$$\phi_i = \tan^{-1} \left[\frac{U_c \tan\alpha_0 + (\dot{y}_i - \dot{y}_{i-1})}{U_c - (\dot{x}_{i-1} - \dot{x}_i)} \right] \quad (4)$$

and

$$U_{r,i}^2 = [U_c \tan\alpha_0 + (\dot{y}_i - \dot{y}_{i-1})]^2 + [U_c - (\dot{x}_{i-1} - \dot{x}_i)]^2 . \quad (5)$$

The force coefficients are given by

$$C_{x,i} = \frac{U_{r,i}^2}{U_c^2} [C_L \sin\phi_i + C_D \cos\phi_i] \quad (6a)$$

and

$$C_{y,i} = \frac{U_{r,i}^2}{U_C^2} [C_L \cos \phi_i + C_D \sin \phi_i] . \quad (6b)$$

The excitation forces may, therefore, be expressed as

$$F_{x,i} = \frac{1}{2} \rho U_C^2 A C_{x,i} \quad (7a)$$

and

$$F_{y,i} = \frac{1}{2} \rho U_C^2 A C_{y,i} , \quad (7b)$$

where ρ is the fluid density and A is the convolute tip surface area.

Upon substitution of the expression for ϕ_i into the expressions for the force coefficients one obtains

$$C_{x,i} = \frac{U_{r,i}^2}{U_C^2} \left\{ C_L \sin \left[\tan^{-1} \left(\frac{U_C \tan \alpha_0 + (\dot{y}_i - \dot{y}_{i-1})}{U_C - (\dot{x}_{i-1} - \dot{x}_i)} \right) \right] \right. \\ \left. + C_D \cos \left[\tan^{-1} \left(\frac{U_C \tan \alpha_0 + (\dot{y}_i - \dot{y}_{i-1})}{U_C - (\dot{x}_{i-1} - \dot{x}_i)} \right) \right] \right\} \quad (8a)$$

and

$$C_{y,i} = \frac{U_{r,i}^2}{U_C^2} \left\{ C_L \cos \left[\tan^{-1} \left(\frac{U_C \tan \alpha_0 + (\dot{y}_i - \dot{y}_{i-1})}{U_C - (\dot{x}_{i-1} - \dot{x}_i)} \right) \right] \right. \\ \left. + C_D \sin \left[\tan^{-1} \left(\frac{U_C \tan \alpha_0 + (\dot{y}_i - \dot{y}_{i-1})}{U_C - (\dot{x}_{i-1} - \dot{x}_i)} \right) \right] \right\} . \quad (8b)$$

Upon introducing the trigonometric identities

$$\sin(\tan^{-1} \theta) = \frac{\theta}{1 + \theta^2}$$

and

$$\cos(\tan^{-1}\theta) = \frac{1}{1 + \theta^2}$$

the force coefficients, with some rearranging, become

$$C_{x,i} = \frac{U_{r,i}^2}{U_c^2} \left\{ C_L \left[\frac{U_c \tan \alpha_0 + (\dot{y}_i - \dot{y}_{i-1})}{U_c - (\dot{x}_{i-1} - \dot{x}_i)} \right] + C_D \right\} \\ \left\{ 1 + \left[\frac{U_c \tan \alpha_0 + (\dot{y}_i - \dot{y}_{i-1})}{U_c - (\dot{x}_{i-1} - \dot{x}_i)} \right]^2 \right\}^{-1/2} \quad (9a)$$

and

$$C_{y,i} = \frac{U_{r,i}^2}{U_c^2} \left\{ C_L + C_D \left[\frac{U_c \tan \alpha_0 + (\dot{y}_i - \dot{y}_{i-1})}{U_c - (\dot{x}_{i-1} - \dot{x}_i)} \right] \right\} \\ \left\{ 1 + \left[\frac{U_c \tan \alpha_0 + (\dot{y}_i - \dot{y}_{i-1})}{U_c - (\dot{x}_{i-1} - \dot{x}_i)} \right]^2 \right\}^{-1/2} \quad (9b)$$

Use of Equation (5) into Equations (9a) and (9b) yields the desired expressions for the force coefficients as [9]

$$C_{x,i} = \frac{1}{U_c^2} \left\{ [U_c \tan \alpha_0 + (\dot{y}_i - \dot{y}_{i-1})]^2 + [U_c - (\dot{x}_{i-1} - \dot{x}_i)]^2 \right\}^{1/2} \\ \{ C_L [U_c \tan \alpha_0 + (\dot{y}_i - \dot{y}_{i-1})] + C_D [U_c - (\dot{x}_{i-1} - \dot{x}_i)] \} \quad (10a)$$

and

$$C_{y,i} = \frac{1}{U_c^2} \left\{ [U_c \tan \alpha_0 + (\dot{y}_i - \dot{y}_{i-1})]^2 + [U_c - (\dot{x}_{i-1} - \dot{x}_i)]^2 \right\}^{1/2} \\ \{ C_L [U_c - (\dot{x}_{i-1} - \dot{x}_i)] + C_D [U_c \tan \alpha_0 + (\dot{y}_i - \dot{y}_{i-1})] \} \quad (10b)$$

The excitation forces may now be written as

$$F_{x,i} = \frac{1}{2} \rho A \{ [U_C \tan \alpha_0 + (\dot{y}_i - \dot{y}_{i-1})]^2 + [U_C - (\dot{x}_{i-1} - \dot{x}_i)]^2 \}^{1/2} \quad (11a)$$

$$\{ C_L [U_C \tan \alpha_0 + (\dot{y}_i - \dot{y}_{i-1})] + C_D [U_C - (\dot{x}_{i-1} - \dot{x}_i)] \}$$

and

$$F_{y,i} = \frac{1}{2} \rho A \{ [U_C \tan \alpha_0 + (\dot{y}_i - \dot{y}_{i-1})]^2 + [U_C - (\dot{x}_{i-1} - \dot{x}_i)]^2 \}^{1/2} \quad (11b)$$

$$\{ C_L [U_C - (\dot{x}_{i-1} - \dot{x}_i)] + C_D [U_C \tan \alpha_0 + (\dot{y}_i - \dot{y}_{i-1})] \} .$$

It may be noted that in addition to fluctuations in the excitation force due to convolute motion, there is also a fluctuation expressed quantitatively due to vortex shedding that was suggested in a qualitative way previously by others. As the vortex moves across the region of highest pressure on the convolute tip, the pressure is reduced. After the vortex has been shed the high pressure region is reestablished, thus producing an "on-off-on" type of fluctuation in the force which is already varying with convolute motion.

Equations (11a) and (11b) are to be incorporated as excitation forces in the vibration model that represents the dynamic force balance of the bellows.

The Lumped Parameter Vibration Model

The development of an expression for the excitation force acting on an individual convolute suggests the need for a mechanical model which allows both longitudinal and transverse motion of the convolute. In order to develop such a model the bellows is divided into discrete mass elements such as the

one shown in Figure 9. By considering longitudinal and transverse motion of this mass element and the elements adjacent to it, a two dimensional vibration model is developed. This is illustrated in Figure 10, where $F_{D,x}$ and $F_{D,y}$ are damping forces which represent such effects as sliding between plies of the bellows and internal frictional damping. Viscous damping is not shown in the illustration, since the damping effect produced by the fluid surrounding the convolute is already included in the expression for the excitation. k_x and k_y are material spring constants, m_m the material mass of one element and m_f the fluid mass of one element. These components of the lumped model are further defined elsewhere in this report.

From the vibration model illustrated in Figure 10 a system of equations describing the motion of the convolutions must be developed. This system must include all of the lumped parameters and effects described above. The system, when solved, must also provide displacement as a function of time for each of the convolute tips.

The development of the equations governing the system behavior results in two times the number of convolutions coupled, nonlinear, ordinary, differential equations. These equations are derived by performing a force balance on the discrete mass element shown in Figure 11(a). The force balance gives

$$\Sigma F_x = F_{x,i} + F_{D,x} \operatorname{sgn}(\dot{x}_i) + k_x(x_{i+1} - 2x_i + x_{i-1}) = (m_m + m_f)\ddot{x}_i ,$$

which upon rearranging becomes

$$(m_m + m_f)\ddot{x}_i - F_{D,x} \operatorname{sgn}(\dot{x}_i) + k_x(2x_i - x_{i+1} - x_{i-1}) = F_{x,i} . \quad (12)$$

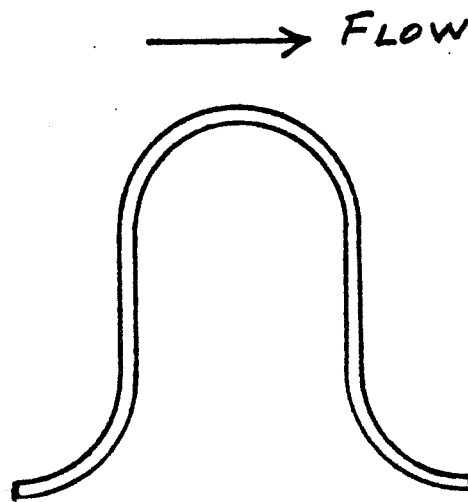


Figure 9. Convolute Representing One Discrete Mass.

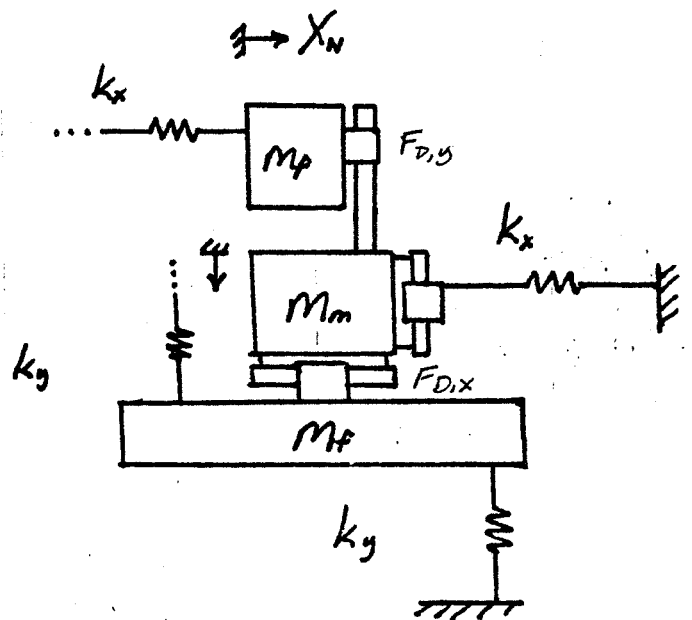
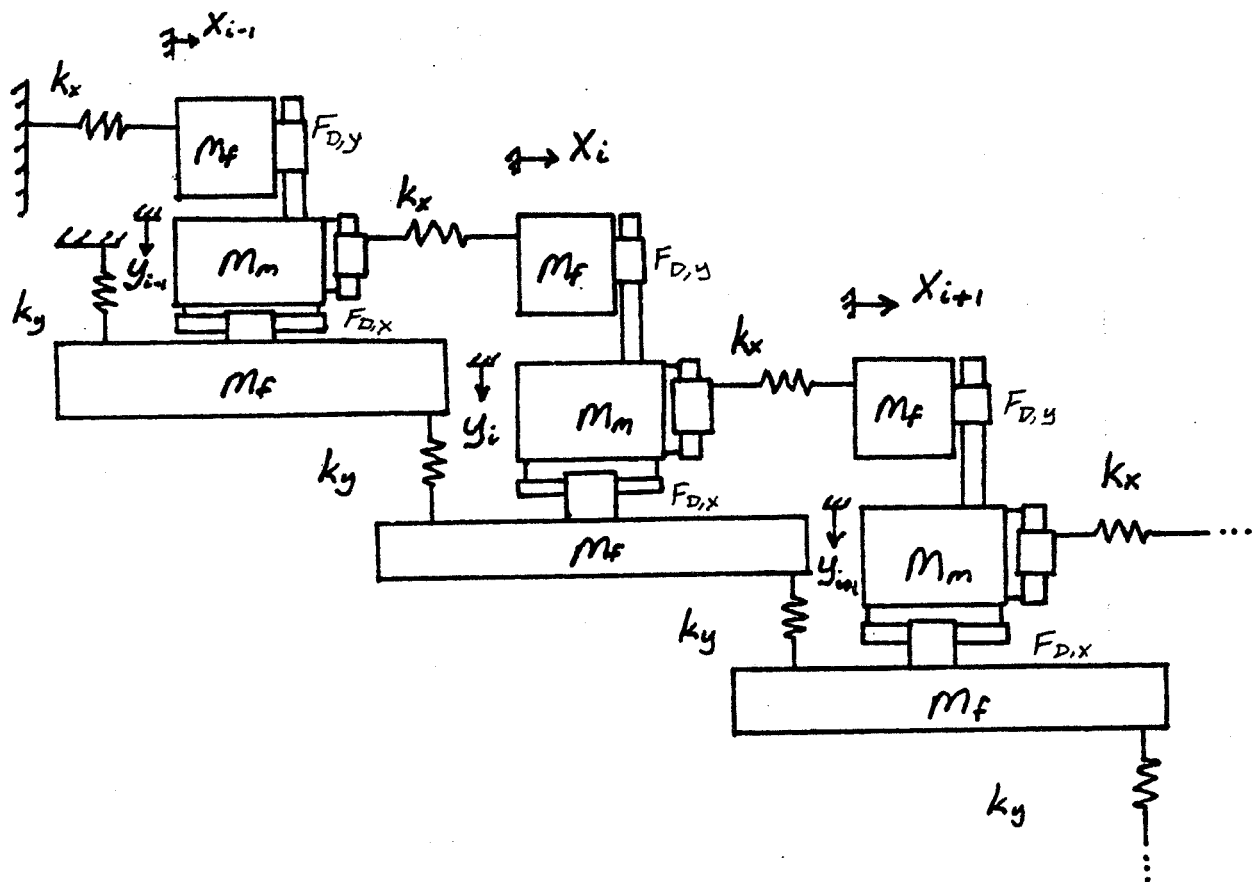


Figure 10. Vibration Model.

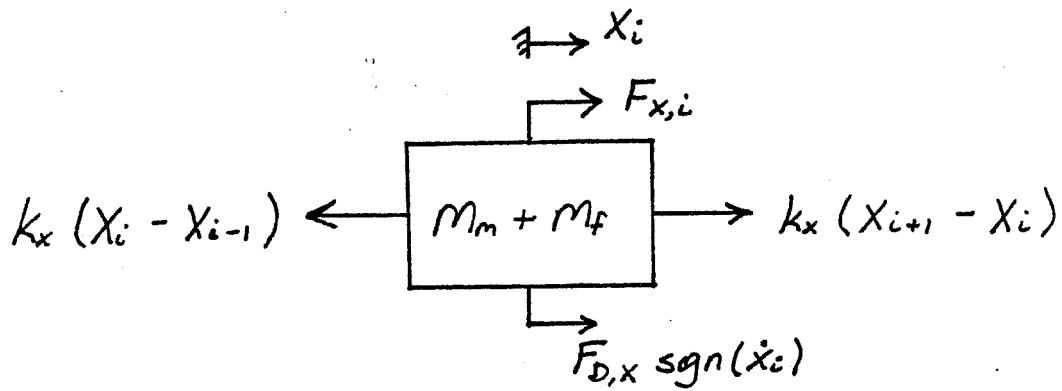


Figure 11a. Force Balance Along x-direction.

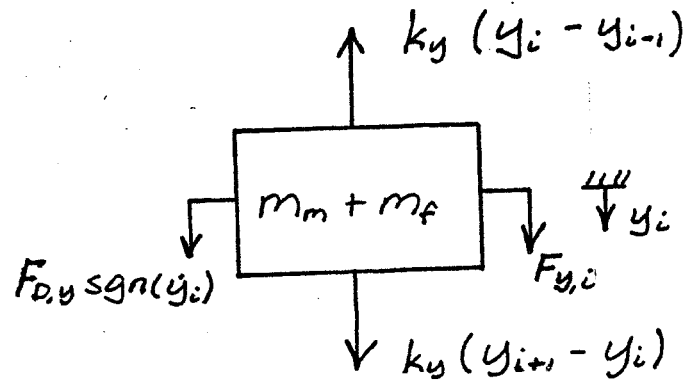


Figure 11b. Force Balance Along y-direction.

The force balance in the transverse direction also may be performed on the element shown in Figure 11(b). This gives

$$\Sigma F_y = F_{y,i} + F_{D,y} \operatorname{sgn}(\dot{y}_i) + k_y(y_{i+1} - 2y_i + y_{i-1}) = (m_m + m_f)\ddot{y}_i$$

Once again, rearrangement gives

$$(m_m + m_f)\ddot{y}_i - F_{D,y} \operatorname{sgn}(\dot{y}_i) + k_y(2y_i - y_{i+1} - y_{i-1}) = F_{y,i} \quad (13)$$

Upon substitution of the previously determined expressions for $F_{x,i}$ and $F_{y,i}$ the system governing equations become

$$\begin{aligned} & (m_m + m_f)\ddot{x}_i - F_{D,x} \operatorname{sgn}(\dot{x}_i) + 2k_x x_i - k_x x_{i+1} - k_x x_{i-1} \\ & = \frac{1}{2} \rho A \{ [U_C \tan \alpha_0 + (\dot{y}_i - \dot{y}_{i-1})]^2 + [U_C - (\dot{x}_{i-1} - \dot{x}_i)]^2 \}^{1/2} \end{aligned} \quad (14)$$

$$\{ C_L [U_C \tan \alpha_0 + (\dot{y}_i - \dot{y}_{i-1})] + C_D [U_C - (\dot{x}_{i-1} - \dot{x}_i)] \}$$

and

$$\begin{aligned} & (m_m + m_f)\ddot{y}_i - F_{D,y} \operatorname{sgn}(\dot{y}_i) + 2k_y y_i - k_y y_{i+1} - k_y y_{i-1} \\ & = \frac{1}{2} \rho A \{ [U_C \tan \alpha_0 + (\dot{y}_i - \dot{y}_{i-1})]^2 + [U_C - (\dot{x}_{i-1} - \dot{x}_i)]^2 \}^{1/2} \end{aligned} \quad (15)$$

$$\{ C_L [U_C - (\dot{x}_{i-1} - \dot{x}_i)] + C_D [U_C \tan \alpha_0 + (\dot{y}_i - \dot{y}_{i-1})] \} ,$$

where each value of i designates a specific convolute. This produces the previously mentioned system of coupled, nonlinear, ordinary, differential

equations.

The solution of this system is sought under the assumption that the bellows is rigidly attached at each end and that the entire system is initially quiescent.

Components of the Lumped Parameter Model

The Fluid Added Mass

As a convolute is displaced it also displaces a certain amount of the fluid flowing through the bellows. This implies that the mass of this fluid must be included in the governing equations as an inertial effect; hence, the $m_f \ddot{x}_i$ and $m_f \ddot{y}_i$ terms. Each convolution has an instantaneous configuration ranging between the two extremes shown in Figure 12(a). This suggests that the fluid added mass varies with instantaneous longitudinal position much more than transverse position. The expression for the fluid added mass will therefore be a function of the longitudinal position of adjacent convolutes. With the geometry defined in Figure 12(b) an expression may be developed for the fluid mass. For example, the instantaneous cavity width and length of the straight section are given by

$$\delta = \delta_0 + (x_i - x_{i-1}) \quad (16)$$

and

$$l = l_0 + \frac{\pi}{2} (x_{i-1} - x_i) . \quad (17)$$

With this information the areas A_1 , A_2 , and A_3 may be determined and swept around the bellows to yield the volume of the fluid added mass. Multiplying this volume by the fluid density, ρ , yields the expression for the fluid added mass, m_f , as

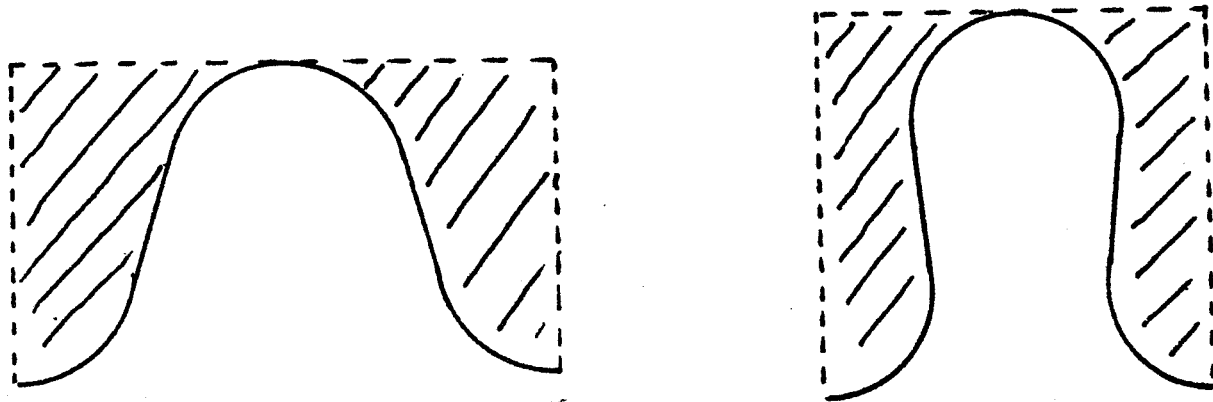


Figure 12a. Instantaneous Fluid Mass Configurations.

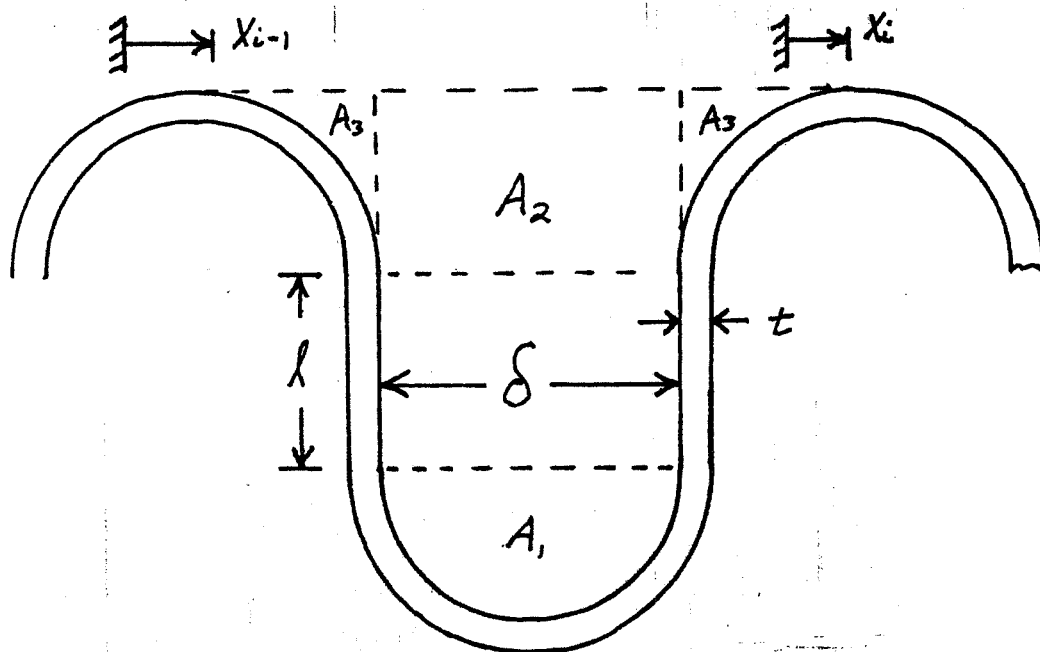


Figure 12b. Geometry to Compute Fluid Mass.

$$m_f = \pi \rho D_m \left\{ \frac{\pi}{8} (\delta_0 + (x_i - x_{i-1}))^2 + (\delta_0 + (x_i - x_{i-1})) \left[\ell_0 + \frac{1}{2} \delta_0 + t + \frac{1-\pi}{2} (x_i - x_{i-1}) \right] + \left(\frac{4-\pi}{2} \right) \left[\frac{1}{2} (\delta_0 + (x_i - x_{i-1})) + t \right]^2 \right\} . \quad (18)$$

Here, D_m is the mean bellows diameter. Since this expression is multiplied by \ddot{x}_i and \ddot{y}_i in the governing equations it introduces additional nonlinear effects into the system of governing equations.

The Material Mass

Each discrete mass in the vibration model is composed of the material mass of one convolution as well as the fluid added mass. Having determined an expression for the fluid mass added to one convolute in motion, an evaluation of the material mass which composes one convolute may also be obtained.

A cross-section of one convolute is illustrated in Figure 13. The area of this cross-section is given by

$$\text{AREA} = [(2\pi + 4)a + 2h]t \quad (19)$$

The volume of material may then be determined by sweeping this area around the bellows mean diameter to yield

$$\text{VOLUME} = \pi D_m [(2\pi - 4)a + 2h]t . \quad (20)$$

The material mass of one convolute, m_m , is determined by multiplying this volume by the material density, ρ_m . This gives

$$m_m = \pi D_m \rho_m [(2\pi - 4)a + 2h]t . \quad (21)$$

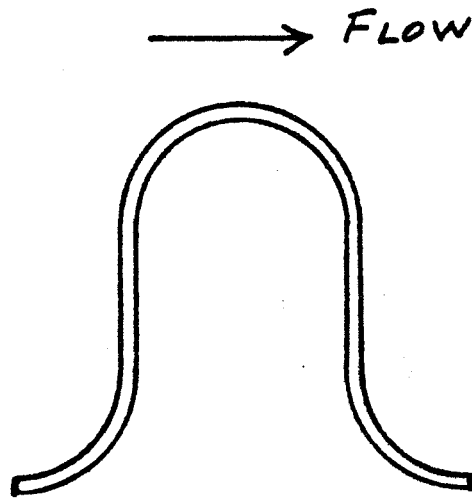


Figure 13. Convolute Geometry to Calculate Material Mass.

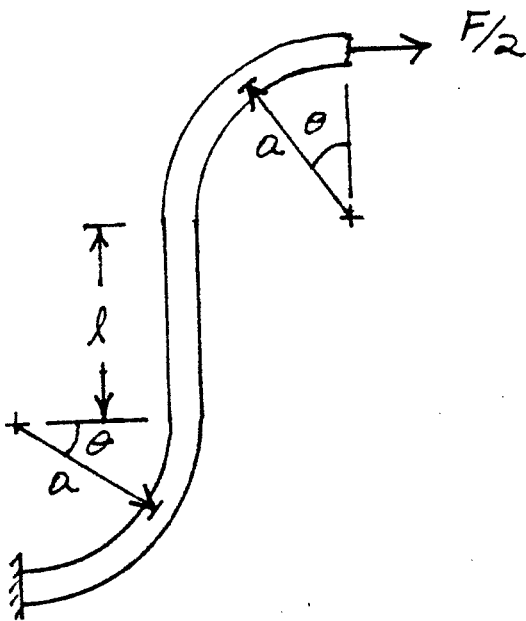


Figure 14a. Configuration to Calculate Spring Constant, k_x .

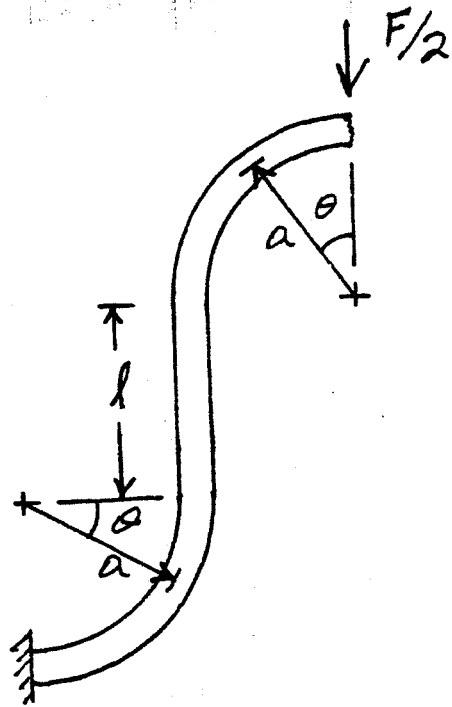


Figure 14b. Configuration to Calculate Spring Constant, k_y .

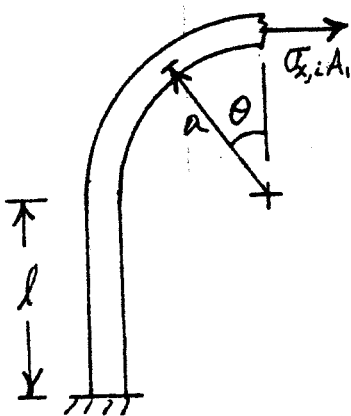


Figure 15a. Geometry to Calculate Convolute Tip Strain Along x-direction.

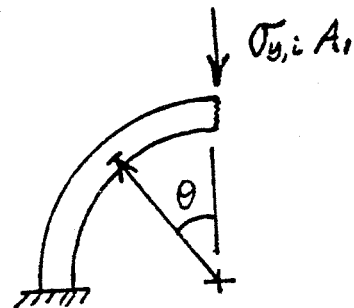


Figure 15b. Geometry to Calculate Convolute Tip Strain Along y-direction.

The Longitudinal Spring Constant, k_x

The longitudinal spring force is the force tending to restore the convolute to its equilibrium position when it has been deformed by a longitudinal displacement. This force is a result of the elasticity of the bellows material. In the vibration model the spring force is represented as a longitudinal spring constant, k_x , multiplied by the displacement of the convolute relative to adjacent convolutes.

An expression for the spring constant can be determined by using the strain energy method along with the theorem of Castigliano. From the geometry illustrated in Figure 14(a) and with a force applied in the longitudinal direction the strain energy of this configuration is given by

$$U = F_x^2 \left\{ \left(\frac{3\pi}{4} - 2 \right) \frac{a^3}{8EI_1} + \frac{\pi}{4} \frac{a}{8EA_1} + \frac{\pi}{4} \frac{a}{8GA_1} + \frac{\ell}{8GA_2} + \frac{a^2 \ell}{8EI_2} \right. \\ \left. + \frac{\pi}{4} \frac{a}{8EA_3} + \frac{\pi}{4} \frac{a}{8GA_3} + \left(\frac{3\pi}{4} + 2 \right) \frac{a^3}{8EI_3} + (2 + \pi) \frac{a^2 \ell}{8EI_3} + \frac{\pi}{2} \frac{a \ell^2}{8EI_3} \right\} . \quad (22)$$

Here, U is the strain energy for the configuration illustrated in Figure 14(a), E is the bellows material modulus of elasticity, and G is the shear modulus. A_1, I_1 , are the cross-sectional area and moment of inertia for the section based on the bellows inside diameter. A_2, I_2 and A_3, I_3 are based on the bellows mean diameter and outside diameter, respectively.

The theorem of Castigliano states that the derivative of the strain energy with respect to an applied force is the displacement of the point of application of the force in the direction of the force. Therefore, the longitudinal displacement of the convolute tip illustrated in Figure 14(a) may be determined as

$$\begin{aligned}
\delta_x = \frac{\partial U}{\partial F_x} = 2F_x \left\{ \left(\frac{3\pi}{4} - 2 \right) \frac{a^3}{8EI_1} + \frac{\pi a}{4 \cdot 8EA_1} + \frac{\pi a}{4 \cdot 8GA_1} + \frac{a}{8GA_2} \right. \\
+ \frac{a^2 \ell}{8EI_2} + \frac{\pi a}{4 \cdot 8EA_3} + \frac{\pi a}{4 \cdot 8GA_3} + \left(\frac{3\pi}{4} + 2 \right) \frac{a^3}{8EI_3} \\
\left. + (2 + \pi) \frac{a^2 \ell}{8EI_3} + \frac{\pi a \ell^2}{2 \cdot 8EI_3} \right\} .
\end{aligned} \tag{23}$$

Since the longitudinal spring constant is the force required to produce a given displacement, the spring constant may be determined as

$$\begin{aligned}
k_x = \frac{F_x}{\delta_x} = \frac{1}{2} \left\{ \left(\frac{3\pi}{4} - 2 \right) \frac{a^3}{8EI_1} + \frac{\pi a}{4 \cdot 8EA_1} + \frac{\pi a}{4 \cdot 8GA_1} + \frac{\ell}{8GA_2} \right. \\
+ \frac{a^2 \ell}{8EI_2} + \frac{\pi a}{4 \cdot 8EA_3} + \frac{\pi a}{4 \cdot 8GA_3} + \left(\frac{3\pi}{4} + 2 \right) \frac{a^3}{8EI_3} \\
\left. + (2 + \pi) \frac{a^2 \ell}{8EI_3} + \frac{\pi a \ell^2}{2 \cdot 8EI_3} \right\}^{-1} .
\end{aligned} \tag{24}$$

The Transverse Spring Constant, k_y

The transverse spring constant may be determined in a manner analogous to the method used for determining the longitudinal spring constant. The strain energy for the configuration illustrated in Figure 14(b) is found to be

$$\begin{aligned}
U = F_y^2 \left\{ \frac{\pi a^3}{4 \cdot 8EI_1} + \frac{\pi a}{4 \cdot 8EA_1} + \frac{\pi a}{4 \cdot 8GA_1} + \frac{a^2 \ell}{8EI_2} + \frac{\ell}{8EA_2} \right. \\
\left. + \left(\frac{9\pi}{4} - 4 \right) \frac{a^3}{8EI_3} + \frac{\pi a}{4 \cdot 8EA_3} + \frac{\pi a}{4 \cdot 8GA_3} \right\} .
\end{aligned} \tag{25}$$

By the theorem of Castigliano the transverse displacement is given as

$$\delta_y = \frac{\partial U}{\partial F_y} = 2F_y \left\{ \frac{\pi}{4} \frac{a^3}{8EI_1} + \frac{\pi}{4} \frac{a}{8EA_1} + \frac{\pi}{4} \frac{a}{8GA_1} + \frac{a^2 \ell}{8EI_2} \right. \\ \left. + \frac{\ell}{8EA_2} + \left(\frac{9\pi}{4} - 4 \right) \frac{a^3}{8EI_3} + \frac{\pi}{4} \frac{a}{8EA_3} + \frac{\pi}{4} \frac{a}{8GA_3} \right\} . \quad (26)$$

The transverse spring constant may now be determined as

$$k_y = \frac{F_y}{\delta_y} = \frac{1}{2} \left\{ \frac{\pi}{4} \frac{a^3}{8EI_1} + \frac{\pi}{4} \frac{a}{8EA_1} + \frac{\pi}{4} \frac{a}{8GA_1} + \frac{a^2 \ell}{8EI_2} \right. \\ \left. + \frac{\ell}{8EA_2} + \left(\frac{9\pi}{4} - 4 \right) \frac{a^3}{8EI_3} + \frac{\pi}{4} \frac{a}{8EA_3} + \frac{\pi}{4} \frac{a}{8GA_3} \right\}^{-1} . \quad (27)$$

III. SOLUTIONS IN THE TIME AND FREQUENCY DOMAINS

Solution of the Governing Equations In the Time Domain

The bellows vibrational response to flow excitation is obtained by solving the system of governing equations for the displacements. Since an analytical solution to this system is not known a numerical solution to be executed by computer must be chosen. In problems where the range of integration is considerable, the numerical method employed must be stable and/or relatively stable to obtain an accurate solution. Also, in a vibration problem where the motion is to be studied over a substantial number of oscillations, a method having a small per-step truncation error should be used in order to minimize the cumulative error.

Upon consideration of these requirements, a "predictor - modifier - corrector" method called Hamming's Method was selected as the solution technique [10]. Hamming's Method is both stable and relatively stable and results in small per-step truncation errors.

The iteration algorithm for a differential equation of the form

$$y' = f(y,t) \quad (28a)$$

may be stated as the predicted value of y at $t + 1$:

$$P(y_{t+1}) = y_{t-3} + \frac{4h}{3} [2y'_t - y'_{t-1} + 2y'_{t-2}] \quad (28b)$$

The modified value

$$M(y_{t+1}) = P(y_{t+1}) - \frac{112}{121} [P(y_t) - C(y_t)] \quad (28c)$$

The corrected value

$$C(y_{t+1}) = \frac{1}{8} \{9y_t - y_{t-2} + 3h[m(y'_{t+1}) + 2y'_t - y'_{t-1}]\} \quad (28d)$$

The final value

$$F(y_{t+1}) = C(y_{t+1}) + \frac{9}{121} [P(y_{t+1}) - C(y_{t+1})]. \quad (28e)$$

Here, h is the time step used in the iteration procedure.

As can be seen from these equations Hamming's Method also has the advantage of being relatively efficient in terms of computing time, since there is only one function evaluation per time step. A disadvantage, however, is that Hamming's Method is not self-starting. It requires solution values at the first three time steps in order to begin the iteration process.

To provide the necessary solution for the first three time steps, a fourth-order Runge-Kutta procedure is employed. While being very inefficient in terms of computing time, the Runge-Kutta procedure does have the advantage of being self-starting.

By starting the iteration with an initially quiescent system, the Runge-Kutta procedure determines the longitudinal and transverse displacements of each convolute tip for the first three time steps. This information is then passed on to Hamming's Method which iterates to 4096 time steps, each step being of 0.01 millisecond duration. The displacement information for the last 2048 time steps is stored as a "data sample" for frequency and fatigue calculations. By choosing the last 2048 time steps the "data sample" is considered far enough from time zero where steady-state vibration is assumed.

With the 0.02048 second sample of steady-state vibration displacement information, a frequency response analysis and strain analysis may be performed. Plots of displacement versus time from this solution are shown in Appendix 1.

Frequency Response

Examination of the displacement versus time plots reveals that both longitudinal and transverse vibrating of an individual convolute are made up of several frequency components. Each of these frequency components contribute to the damage done to the convolute during a given time period. In order to estimate the extent of this damage on each convolute the dominating frequencies of vibration in both the longitudinal and transverse directions must be determined.

With the time-dependent displacement obtained from the solution of the governing equations, a Fourier Analysis may be performed. This analysis yields the frequency response of each convolute in each coordinate direction. The Fourier Analysis is performed by means of the Fast Fourier Transform algorithm which is developed here.

By representing the convolute response as a complex Fourier series one obtains

$$x(t) = \frac{1}{2\pi} \sum_{n=-\infty}^{\infty} X(\omega_n) e^{i\omega_n t} \quad (29a)$$

and

$$y(t) = \frac{1}{2\pi} \sum_{n=-\infty}^{\infty} Y(\omega_n) e^{i\omega_n t} \quad (29b)$$

where $X(\omega) = \int_{-\infty}^{\infty} x(t) e^{-i\omega t} dt$ (30a)

$$Y(\omega) = \int_{-\infty}^{\infty} y(t) e^{-i\omega t} dt \quad (30b)$$

ω_n is a discrete angular frequency and t is time. Recall from the solution of the governing equations that the sampling period, T , and the number of data samples, N , are respectively,

$$T = 0.02048 \text{ second} \quad (31a)$$

$$N = 2048 \text{ samples}$$

Therefore the time step size is

$$\Delta T = \frac{T}{N} \quad (31b)$$

The fundamental frequency, ω_0 , is given by

$$\omega_0 = \frac{2\pi}{T} \quad (31c)$$

and the maximum frequency which may be determined, ω_{\max} , is

$$\omega_{\max} = \frac{2\pi}{\Delta t} = \frac{2\pi}{(T/N)} = N\omega_0 \quad (33d)$$

Define a discrete set of N frequencies at which the convolute response will be determined.

$$\omega_n = n\omega_0 = \frac{2\pi n}{T}; \quad n = 0, 1, 2, \dots, N \quad (32)$$

Since $x(t)$ and $y(t)$ vanish for time less than zero and since they have not been determined for time greater than T , the transform may be approximated as

$$X(\omega) = \int_0^T x(t)e^{-i\omega t} dt \quad (33a)$$

and

$$Y(\omega) = \int_0^T y(t)e^{-i\omega t} dt \quad (33b)$$

If these integrals are approximated by summations, the expressions become

$$X(\omega) = \sum_{m=0}^{N-1} x(t_m) e^{-i\omega t_m} \Delta t \quad (34a)$$

and

$$Y(\omega) = \sum_{m=0}^{N-1} y(t_m) e^{-i\omega t_m} \Delta t \quad (34b)$$

Upon evaluating these transform expressions at discrete frequencies, ω_n , one obtains

$$X(\omega_n) = \frac{T}{N} \sum_{m=0}^{N-1} x(t_m) \exp\left[-i \frac{2\pi mn}{N}\right] \quad (35a)$$

and

$$Y(\omega_n) = \frac{T}{N} \sum_{m=0}^{N-1} y(t_m) \exp[-i \frac{2\pi mn}{N}] . \quad (35b)$$

Let $W_N = \exp[-i \frac{2\pi}{N}]$ to get

$$X(\omega_n) = \frac{T}{N} \sum_{m=0}^{N-1} x(t_m) (W_N)^{nm} \quad (36a)$$

and

$$Y(\omega_n) = \frac{T}{N} \sum_{m=0}^{N-1} y(t_m) (W_N)^{nm} . \quad (36b)$$

Each power of W_N increases the polar angle by $2\pi/N$. After N powers the pattern repeats so it is not necessary to compute all powers. Therefore, define U_k such that

$$U_k = (W_N)^k; \quad 0 < k < N$$

and

(37)

$$U_k = U_{\text{mod}(k,N)}; \quad k > N ,$$

where $\text{MOD}(k,N)$ is the modulus function. The combination of U_k with the previous transform expression yields the equations for the transformed response at discrete frequencies as

$$X(\omega_n) = \frac{T}{N} \sum_{m=0}^{N-1} x(t_m) U_{\text{MOD}(mn,N)} \quad (38a)$$

and

$$Y(\omega_n) = \frac{T}{N} \sum_{m=0}^{N-1} y(t_m) U_{\text{MOD}(mn,N)} . \quad (38b)$$

Note that since $(W_n)^{m(-n)}$ is the complex conjugate of $(W_N)^{mn}$, it is sufficient to evaluate $X(\omega_n)$ and $Y(\omega_n)$ for $n > 0$.

The results of the Fast Fourier Transform are the frequency response plots shown in Appendix 1. With this information the dominant frequencies of both longitudinal and transverse vibration of each convolute may be determined. These dominant frequencies will later be used to assess the cumulative damage effects on each convolute.

IV. CYCLIC STRAIN, DAMAGE AND FATIGUE LIFE

Estimation of Cyclic Strains

The numerical model to calculate fatigue life of bellows is based on obtaining strain amplitude for the cyclic deformation of each convolute. The strain amplitude has to be evaluated at the convolute tip since this is the location at which the bellows is known to fail. A maximum and minimum value for the tip strain resulting from both longitudinal and transverse vibration needs to be determined. Since the strain induced at a point by different mechanisms is additive (same fibres damaged), the maximum tip strain resulting from longitudinal vibration and the maximum tip strain resulting from transverse vibration may be added to get a total maximum convolute tip strain. Likewise, the corresponding minimum strains may be added to get a total minimum convolute tip strain. The strain amplitude may then be determined by the equation:

$$\Delta\epsilon = \frac{\epsilon_{\max} - \epsilon_{\min}}{2} \quad (39)$$

where ϵ is the tip strain and $\Delta\epsilon$ the strain amplitude.

In order to determine an expression for the convolute tip strains resulting from both longitudinal and transverse displacements the strain energy method along with the theorem of Castigliano is used. For longitudinal displacement of the convolute tip it is assumed that the strain energy resulting from the displacement is concentrated in the section of the convolute illustrated in Figure 15(a). The strain energy for this configuration is given by

$$U = (\sigma_{x,i} A_1)^2 \left\{ \left(\frac{3\pi}{8} - 1 \right) \frac{a^3}{EI_1} + \frac{\pi}{8} \frac{a}{A_1 E} + \frac{\pi}{8} \frac{a}{GA_1} + \frac{1}{2} \frac{\lambda a^3}{EI_2} + \frac{1}{2} \frac{\lambda a}{GA_2} \right\}, \quad (40)$$

where, as before, E is the bellows material modulus of elasticity and G is the shear modulus. A_1 and I_1 are the cross-sectional area and the moment of inertia based on the bellows inside diameter. A_2 , I_2 and A_3 , I_3 are based on the bellows mean diameter and outside diameter, respectively.

By applying the theorem of Castigliano the longitudinal displacement of the tip, x_i , may be determined as

$$x_i = \frac{\partial U}{\partial (\sigma_{x,i} A_1)} = 2(\sigma_{x,i} A_1) \left\{ \left(\frac{3\pi}{8} - 1 \right) \frac{a^3}{EI_1} + \frac{\pi}{8} \frac{a}{A_1 E} + \frac{\pi}{8} \frac{a}{GA_1} + \frac{1}{2} \frac{\lambda a^3}{EI_2} + \frac{1}{2} \frac{\lambda a}{GA_2} \right\}. \quad (41)$$

Since $\sigma_{x,i} = E \epsilon_{x,i}$, the displacement may also be expressed

$$x_i = 2(\epsilon_{x,i} EA_1) \left\{ \left(\frac{3\pi}{8} - 1 \right) \frac{a^3}{EI_1} + \frac{\pi}{8} \frac{a}{A_1 E} + \frac{\pi}{8} \frac{a}{GA_1} \right\} \quad (42)$$

$$+ \frac{1}{2} \frac{\ell a^3}{GA_1} + \frac{1}{2} \frac{\ell a^3}{EI_2} + \frac{1}{2} \frac{\ell a}{GA_2} \}$$

and the convolute tip strain may be written as

$$\begin{aligned} \epsilon_{x,i} = \frac{x_i}{2EA_1} \{ & (\frac{3\pi}{8} - 1) \frac{a^3}{EI_1} + \frac{\pi}{8} \frac{a}{A_1 E} + \frac{\pi}{8} \frac{a}{GA_1} \\ & + \frac{1}{2} \frac{\ell a^3}{GA_1} + \frac{1}{2} \frac{\ell a^3}{EI_2} + \frac{1}{2} \frac{\ell a}{GA_2} \}^{-1} . \end{aligned} \quad (43)$$

Since the transverse displacements are smaller than the longitudinal displacements the strain energy resulting from transverse displacements is considered to be concentrated in a smaller section of the convolute. Figure 15(b) is an illustration of this section. Once again the strain energy for this configuration is given by

$$U = (\sigma_{y,i} A_1)^2 \frac{\pi}{8} \left\{ \frac{a^3}{EI_1} + \frac{a}{EA_1} + \frac{a}{GA_1} \right\} \quad (44)$$

and application of Castigliano's theorem gives

$$y_i = \frac{2U}{2(\sigma_{y,i} A_1)} = 2(\sigma_{y,i} A_1) \frac{\pi}{8} \left\{ \frac{a^3}{EI_1} + \frac{a}{EA_1} + \frac{a}{GA_1} \right\} . \quad (45)$$

Upon substituting $\sigma_{y,i} = \epsilon_{y,i} E$ and solving the resulting expression for $\epsilon_{y,i}$, the equation for the convolute tip strain resulting from transverse vibration is obtained as

$$\epsilon_{y,i} = \frac{y_i}{EA_1} \frac{4}{\pi} \left\{ \frac{a^3}{EI_1} + \frac{a}{EA_1} + \frac{a}{GA_1} \right\}^{-1} . \quad (46)$$

As described earlier, the maximum values of $\epsilon_{x,i}$ and $\epsilon_{y,i}$ which occur during the sampling period are added to get a total maximum tip strain, $\epsilon_{i,max}$. The minimum values of $\epsilon_{x,i}$ and $\epsilon_{y,i}$ are also added to yield a total minimum tip strain, $\epsilon_{i,min}$. The convolute tip strain amplitude, $\Delta\epsilon_i$, may then be determined by

$$\Delta\epsilon_i = \frac{1}{2} (\epsilon_{i,max} - \epsilon_{i,min}) . \quad (47)$$

Estimate of Cycles to Failure

A modern approach to characterize the fatigue behavior of materials is to focus on the cyclic strain life [12]. The total strain, ϵ , is considered as having an elastic ϵ_e , and a plastic, ϵ_p , components. Expressed as strain amplitudes, this implies

$$\frac{\Delta\epsilon}{2} = \frac{\Delta\epsilon_e}{2} + \frac{\Delta\epsilon_p}{2} . \quad (48)$$

The elastic strain-life can be expressed as

$$\frac{\Delta\epsilon_e}{2} = \frac{\sigma_a}{E} = \frac{1}{E} \sigma_f' (2N_f)^b , \quad (49)$$

where σ_a and σ_f' , respectively, represent the true stress amplitude and the fatigue strength coefficient, E is the modulus of elasticity, b is the fatigue strength exponent (typically, b varies between -0.05 and -0.12) and N_f is the number of cycles to failure. The plastic strain-life is related by a power function as

$$\frac{\Delta\epsilon_p}{2} = \epsilon_f' (2N_f)^d , \quad (50)$$

where ϵ_f' is the fatigue ductility coefficient and d is the fatigue ductility exponent (typically, d varies between -0.5 and -0.7). The total strain amplitude may thus be expressed as

$$\frac{\Delta\epsilon}{2} = \frac{\sigma_f'}{E} (2N_f)^b + \epsilon_f' (2N_f)^d . \quad (51)$$

This equation is called the strain-life relation and forms the basis for the strain-life approach to predicting fatigue behavior of such material as wrought metals. For thin-walled shells, such as the bellows, N_f is typically taken to be the number of cycles to initiate a crack.

With the strain amplitude for each convolute in hand it is possible to compute the number of cycles to failure for each convolute. For the types of steels from which bellows are commonly made, the equation constants are given by

$$b \approx -0.1$$

$$\sigma_f' \approx 150 \text{ kpsi}$$

$$0.5 < \epsilon_f' < 1 \quad (52)$$

$$\text{and } d \approx -0.7$$

The strain-life relation obviously requires an iterative solution. To accomplish this, simple Newton-Raphson Method has been employed. Since the slope of the strain-life relation is always negative, there should be no

problems with convergence so long as N_f is initially relatively small in the iteration process.

Cumulative Damage and Fatigue Life of Bellows

By estimating the cumulative damage done to each convolute during the sample period an estimation can be made as to which convolute will fail first. The assumption made here is that the convolute undergoes cyclic strain of amplitude $\Delta\epsilon_i$ for the time of the sampling period at each of the dominant frequencies determined by the Fourier Analysis. For example:

- o convolute #3 vibrates with strain amplitude $\Delta\epsilon_3$ at a frequency f_1 for a time equal to the sampling period.
- o convolute #3 then vibrates with strain amplitude $\Delta\epsilon_3$ at frequency f_2 for a time equal to the sampling period
- o etc.

From this approach the cumulative damage done to each convolute during one sampling period can be determined. This is done by use of the Palmgren-Miner linear-cumulative-damage rule [12] which may be stated as

$$d = \frac{2N_1}{2N_{f,1}} = \frac{(\text{Reversals applied at } \sigma_{a1})}{(\text{Reversals to failure at } \sigma_{a1})} , \quad (53)$$

where d = damage. Failure will occur when

$$\sum_i \frac{2N_i}{2N_f} = 1 . \quad (54)$$

In the present model the damage for each convolute during the sampling period may be determined by

$$d_i = \frac{2T(f_{i1} + f_{i2} + \dots + f_{in})}{2 N_{f,i}} \quad (55)$$

Here T is the sampling period, N_{fi} is the cycles to failure for the i^{th} convolute, f_{i1}, \dots, f_{in} are the dominant frequencies of vibration, and d_i is the damage for the i^{th} convolute. Since steady state vibration is assumed to exist, the largest value of d_i corresponds to the convolute which is likely to fail first.

The number of cycles to failure for this convolute is also the cycles to failure for the entire bellows. A failure time window may be determined by dividing the bellows cycles to failure by the maximum and minimum dominant frequencies of the convolute which is first to fail. This defines a minimum time to failure as

$$t_{\min} = \frac{N_f}{f_{i,\max}} \quad (56)$$

and a maximum time to failure as

$$t_{\max} = \frac{N_f}{f_{i,\min}} \quad (57)$$

This t_{\min} and t_{\max} then establish a failure time window.

V. CLOSING REMARKS

In testing the bellows computer program it became apparent that the best results are obtained for bellows with up to five convolutions. For bellows with greater than five convolutions the cycles to failure begins to decrease considerably. Therefore, it is recommended that program BELLOWS be used for bellows with up to five convolutions.

The limitation of the program to give resonable vibration amplitudes for bellows with less than five convolutions is attributed to cumulative displacement effects in the springs connecting the discrete masses of the mechanical model. For more than five convolutions the displacements in each consecutive spring adds to eventually produce unreasonable convolute tip displacement. Rather than introducing artificial damping into the governing equations to control these amplitudes, it was decided to limit the model to a five convolution model. Additional effects due to stress wave propagations in bellows with large number of convolutions need to be examined further in future research.

For bellows with differing number of convolutions the interaction between the convolutes results in the strain energy being concentrated in a smaller or larger volume of the convolute. Fewer convolutions result in the strain energy being concentrated in a smaller volume near the convolute tip. To incorporate this effect into the model a factor multiplying the equations for strain calculation has been introduced. The strain multiplying factor varies linearly with the number of convolutions and its determination is internal to the computer program.

A thorough literature search into the effects of sliding damping between plys and internal frictional damping did not yield sufficient information to explicitly incorporate these effects into the model. Just the same such

effects do exist and were included in the model via damping forces. A comparison of calculated fatigue life cycles with measured values [2] indicate very encouraging agreements. The computer calculations were made for equivalent test conditions and bellows specifications to those used in the experiments, except that the number of convolutions used in the model was less than or equal to five. The agreement between the two indicated in Tables 1 and 2 is within an order of magnitude. It is concluded therefore that within the scope of its application, the model presented in this study is quite satisfactory.

Table 1 Computer Results

Bellows Number	# Convolutes in Model	Flow Velocity (ft/s)	Cycles to Fail (10^6)	Min. Time to Fail (sec)	Max. Time to Fail (sec)
5028	5	35	2.9	979.	11,747.
5028	5	50	210.	77,851.	856,362.
5028	5	65	6.7	2482.	27,301.
5013	3	35	0.67	651.	4556.
5013	3	50	0.056	63.8	383.
5005	3	35	0.33	285.	1708.
5005	3	50	0.025	24.5	171.2

Table 2. MSFC Tests [2]

Bellows Number	Flow Velocity (ft/s)	Cycles to Fail (10^6)	Time to Fail (sec)
5028	65.8	-----	787.
5028	66.6	.16	150.
5013	50	1.3	2007 - 2027
5013	45	.47 - .48	749 - 760
5005	33.2	.78 - .79	1841 - 1863
5005	65.2	-----	75 - 100

VI. BIBLIOGRAPHY

1. Johnson, J. E., Doffenbaugh, D. M., Astleford, W. J. and Gerlach, C. R., "Bellows Flow-Induced Vibrations", Final Report, Contract No. NAS8-31994, Southwest Research Institute, October 1979.
2. Gerlach, C. R., Tygielski, P. J., Smyly, H. M., "Bellows Flow-Induced Vibrations", Report number NASATM 82556, Marshall Space Flight Center, 1983.
3. Desai, P. V., Wu, X. F., "Flow-Induced Vibrations in Flexible Components of Space Shuttle Feed Systems", Project Number E25-605, 1984.
4. Naudascher, E., "From Flow Stability to Flow-Induced Excitation," Proc. ASCE., J. Hydraulics Div., Vol. 93, No. HY4, Proc. Paper 5336, July 1967.
5. Rockwell, D., "Prediction of Oscillation Frequencies for Unstable Flow Past Cavities", ASME J. Fluids Engineering, Vol. 99, 1977, pp. 294-300.
6. Haugen, R. L., Dhanak, A. M., "Momentum Transfer in Turbulent Separated Flow Past a Rectangular Cavity", Journal of Applied Mechanics, Sept. 1966.
7. Yang, W. J., "Forced Convection Heat Transfer in Interrupted Compact Surfaces", ASME JSME Thermal Engineering Joint Conference, Vol. 3, pp. 105-109, 1983.
8. Eastop, T. D., Turner, J. R., "Air Flow Around Three Cylinders at Various pitch-to-diameter Ratios for Both a Longitudinal and a Transverse Arrangement", Trans. Inst. of Chem. E., Vol. 60, 1982.
9. Desai, P. V., Thornhill, L., "Fatigue Behavior of Flexhoses and Bellows Due to Flow-Induced Vibrations," Interim Report for NASA/KSC, NAG10=0017, July 1985.
10. Meirovitch, Leonard, "Elements of Vibration Analysis", McGraw-Hill Co., New York, 1975.
11. James, M. L., Smith, G. M. and WOLFORD, J. C. Applied Numerical Methods for Digital Computation, Harper and Row, 1977.
12. Socie, D. F., Mitchell, M. R. and Caulfield, E. M., "Fundamentals of Modern Fatigue Analysis", Fracture Control Program Report #26, College of Engineering, University of Illinois, January 1978.
13. Blevins, Robert D., "Flow-Induced Vibrations", Van Nostrand Reinhold Co., New York, 1977.

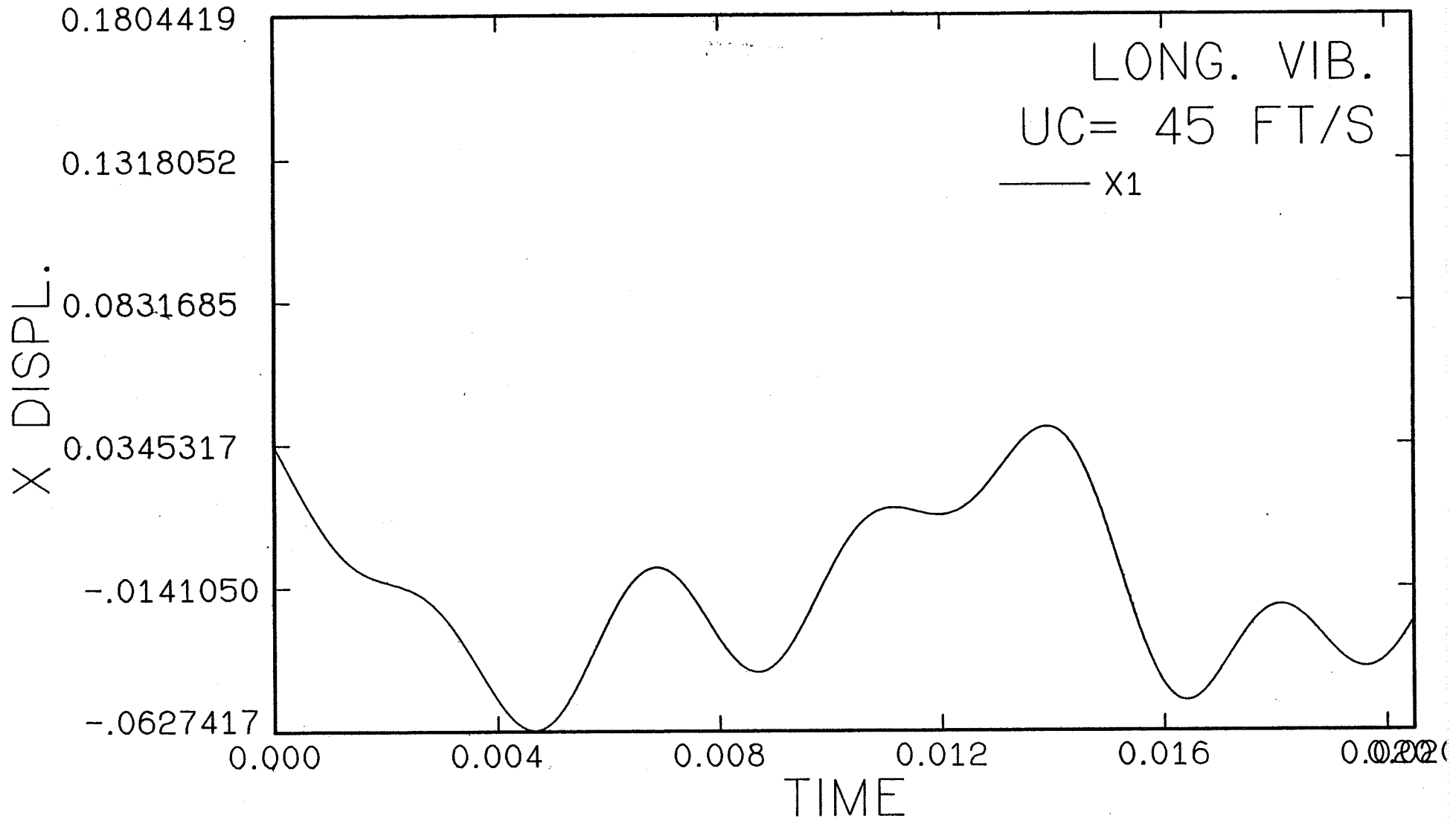
APPENDIX I

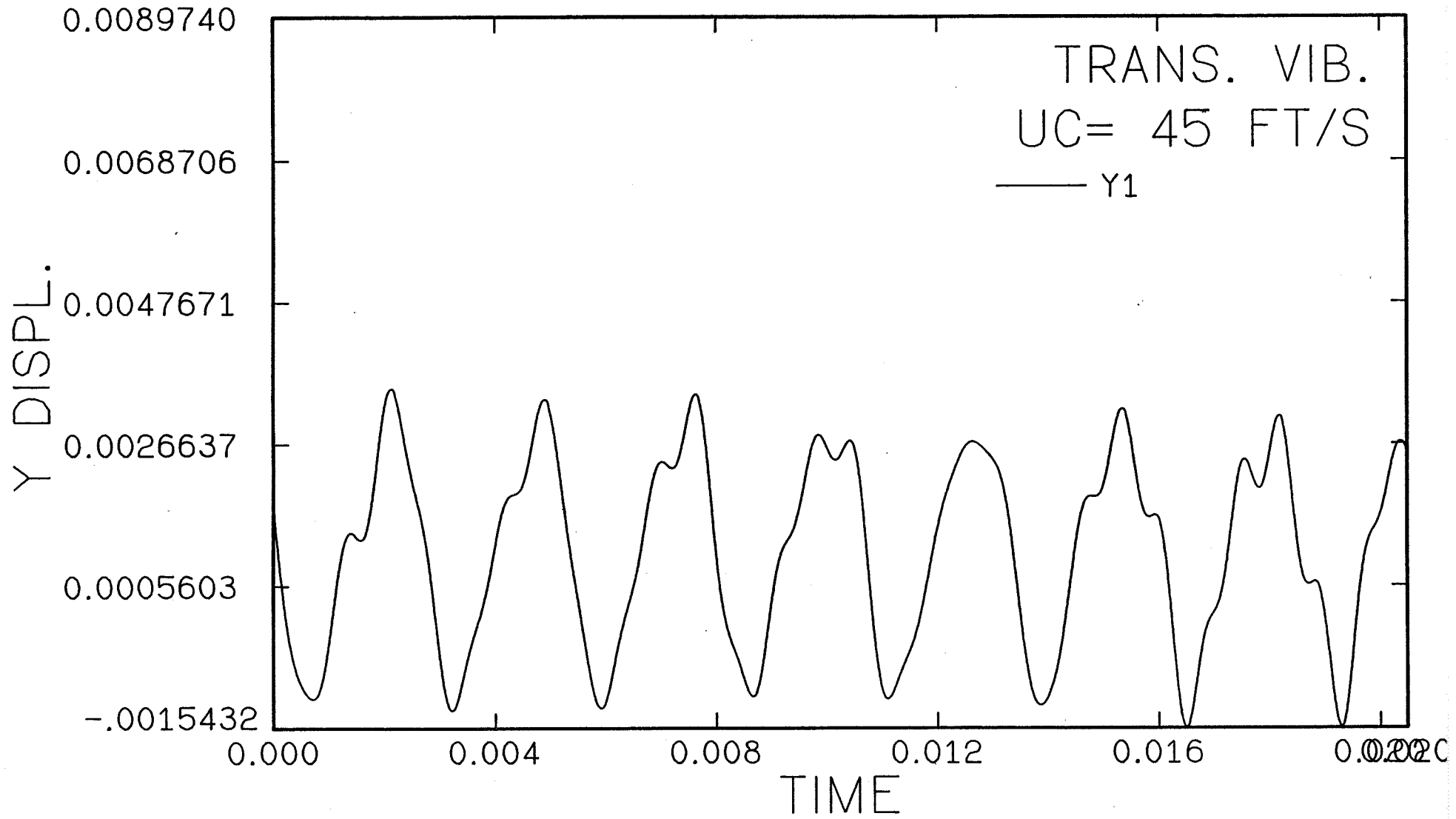
SAMPLE PLOTS FOR TIME AND FREQUENCY DOMAIN RESPONSES

In the time response plots, the core velocity, U_c , is taken as 45 ft/sec. The horizontal axis indicates time in seconds and the vertical axis indicates displacement in inch. x and y , respectively, indicate longitudinal and transverse vibrations displacements. Subscripts on x and y indicate the data for the particular convolution number.

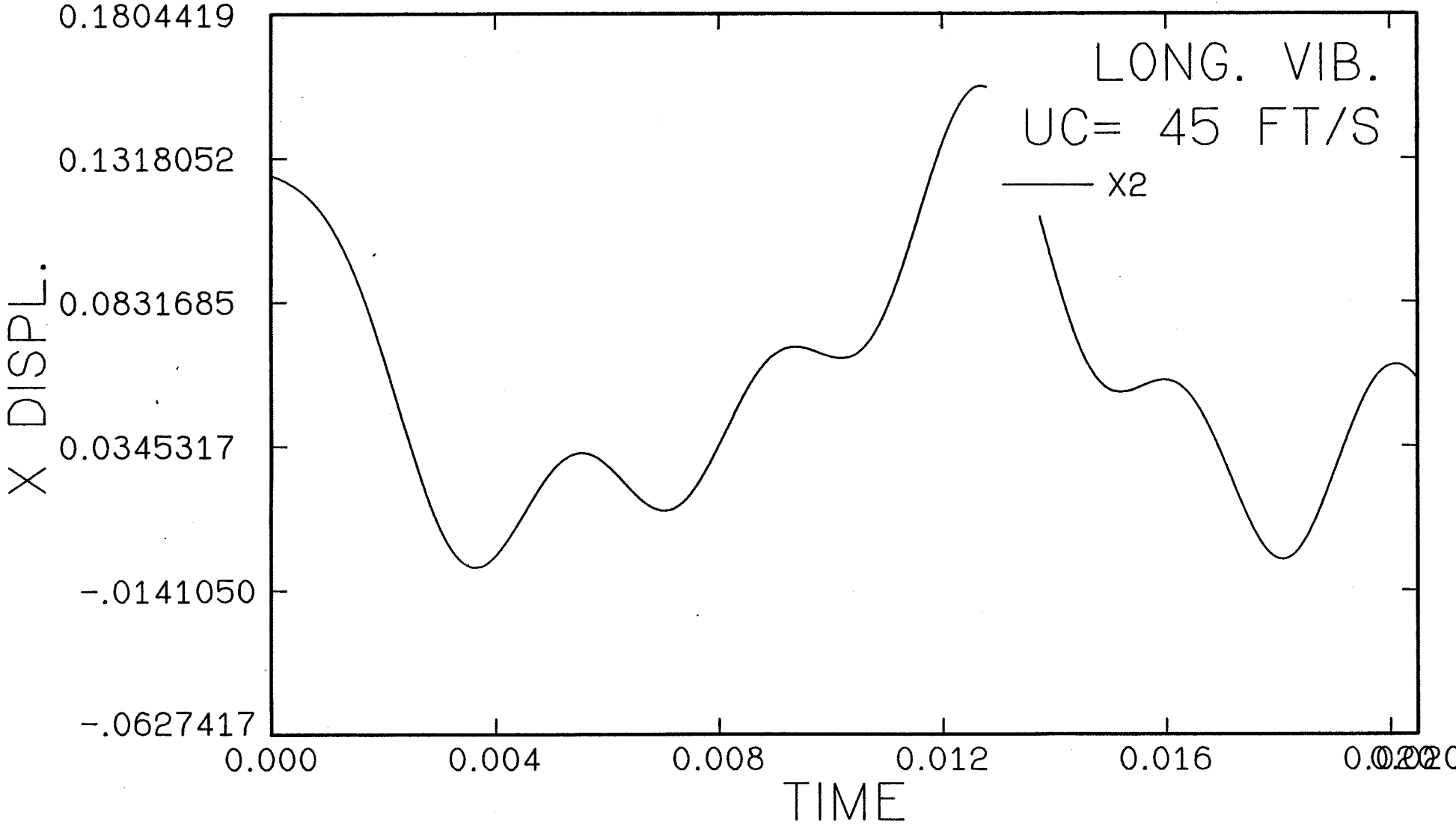
In the frequency response plots, the vertical axis indicates the Fourier-transformed displacements and the horizontal axis indicates frequency in radians/second. The core velocity, U_c , for all plots is 45 ft/sec.

- 45 -

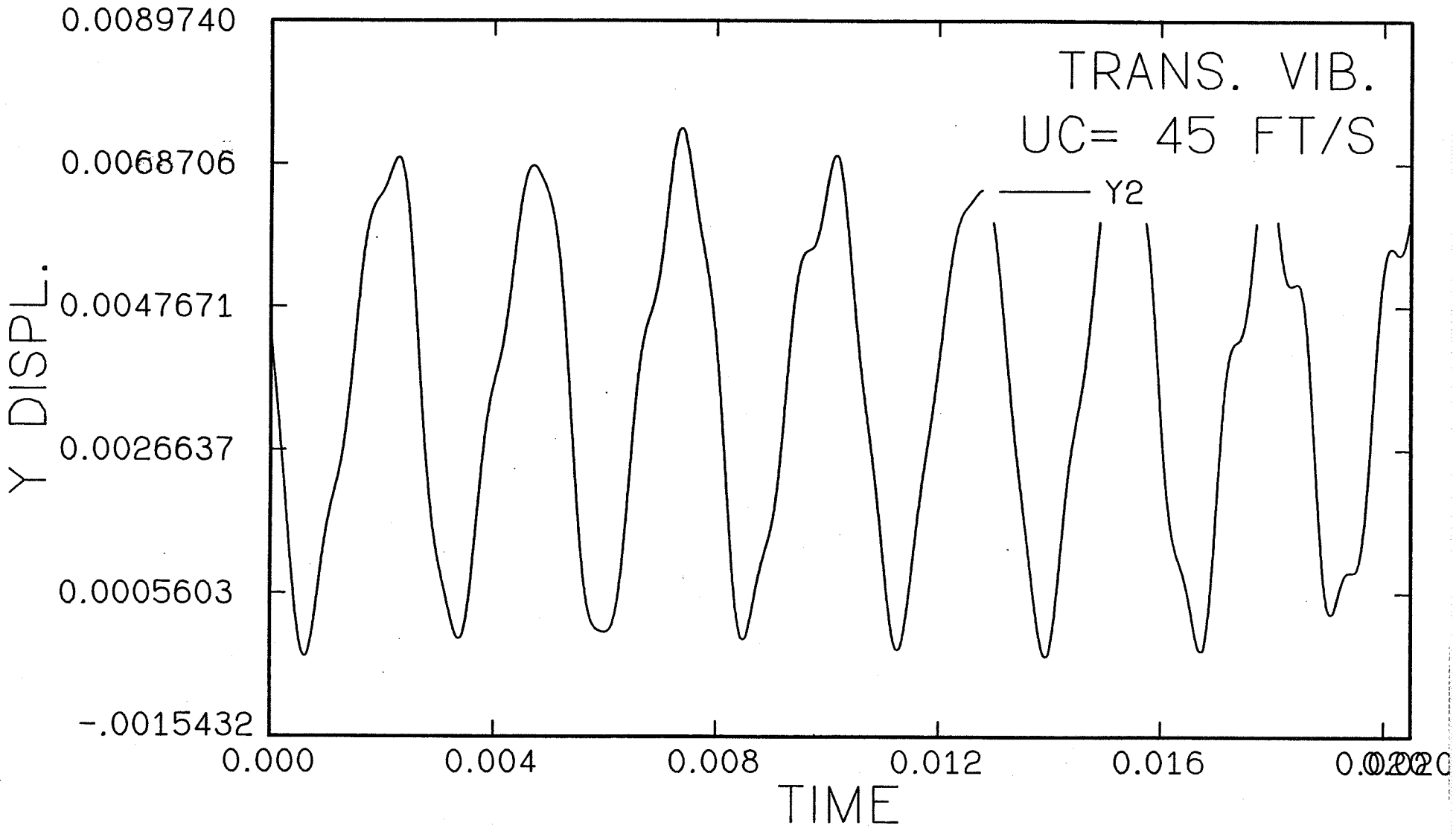


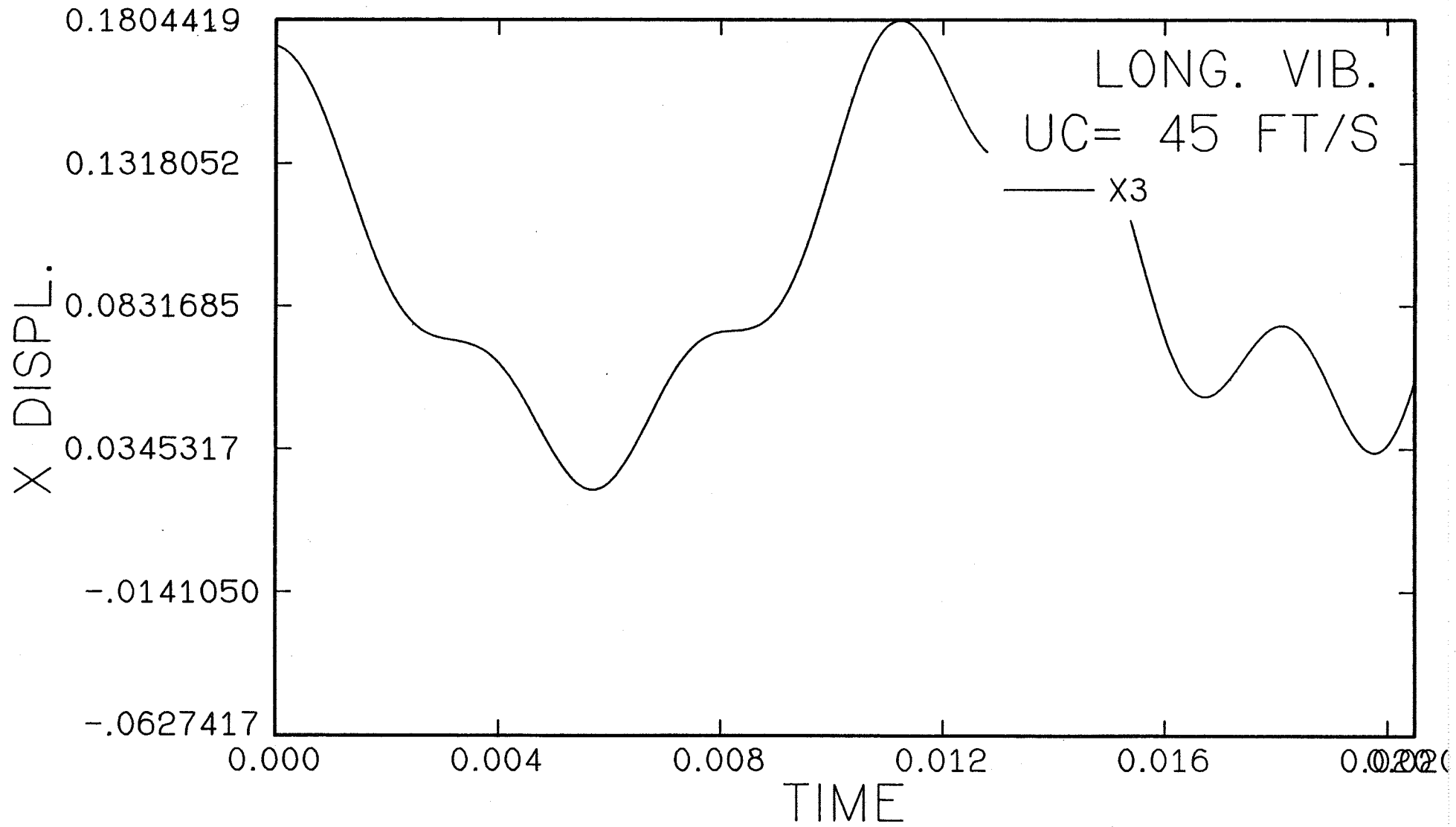


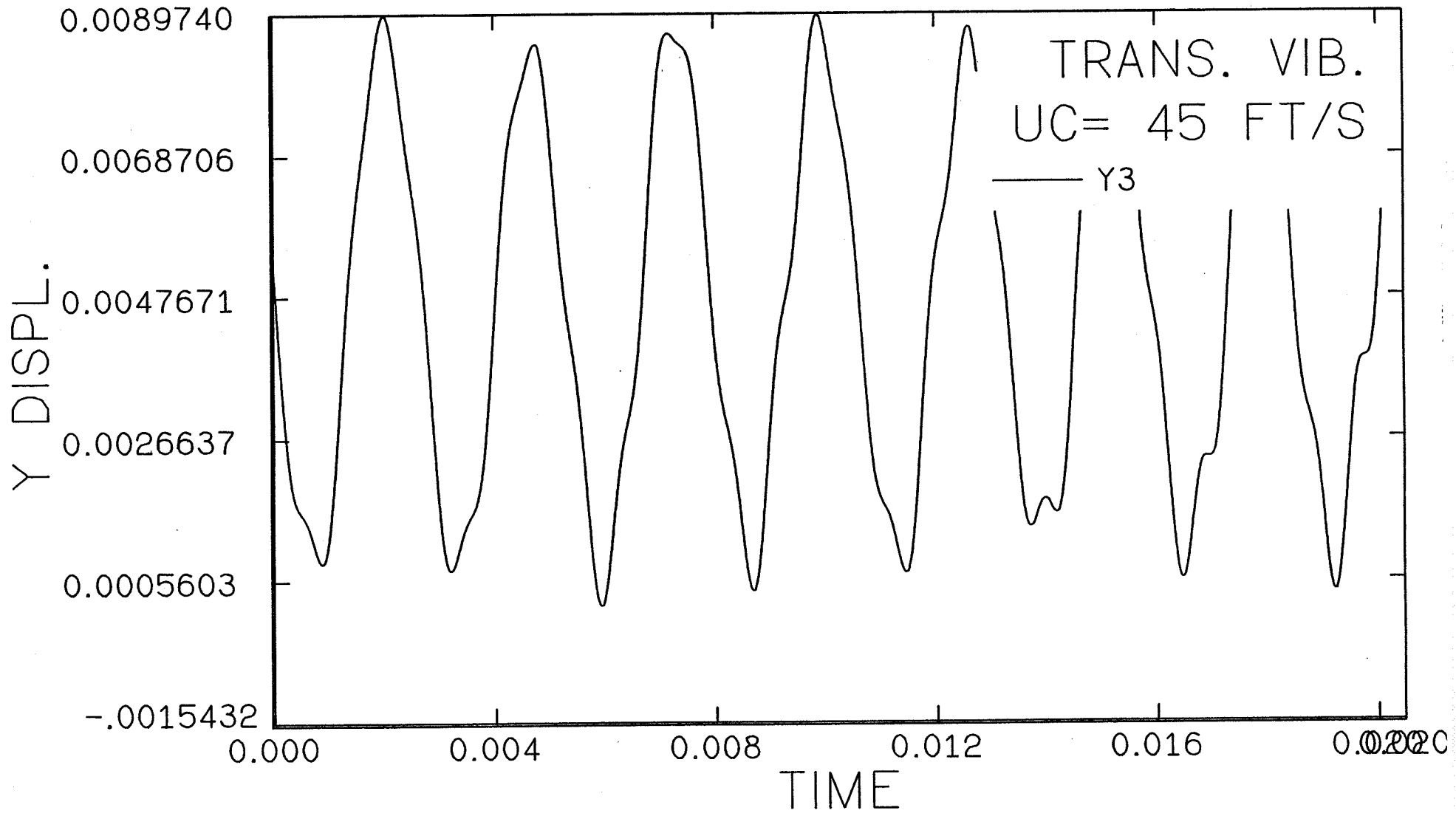
- 47 -



- 48 -







- 15 -

X DISPL.

0.1804419

0.1318052

0.0831685

0.0345317

-0.0141050

-0.0627417

0.000

0.004

0.008

0.012

0.016

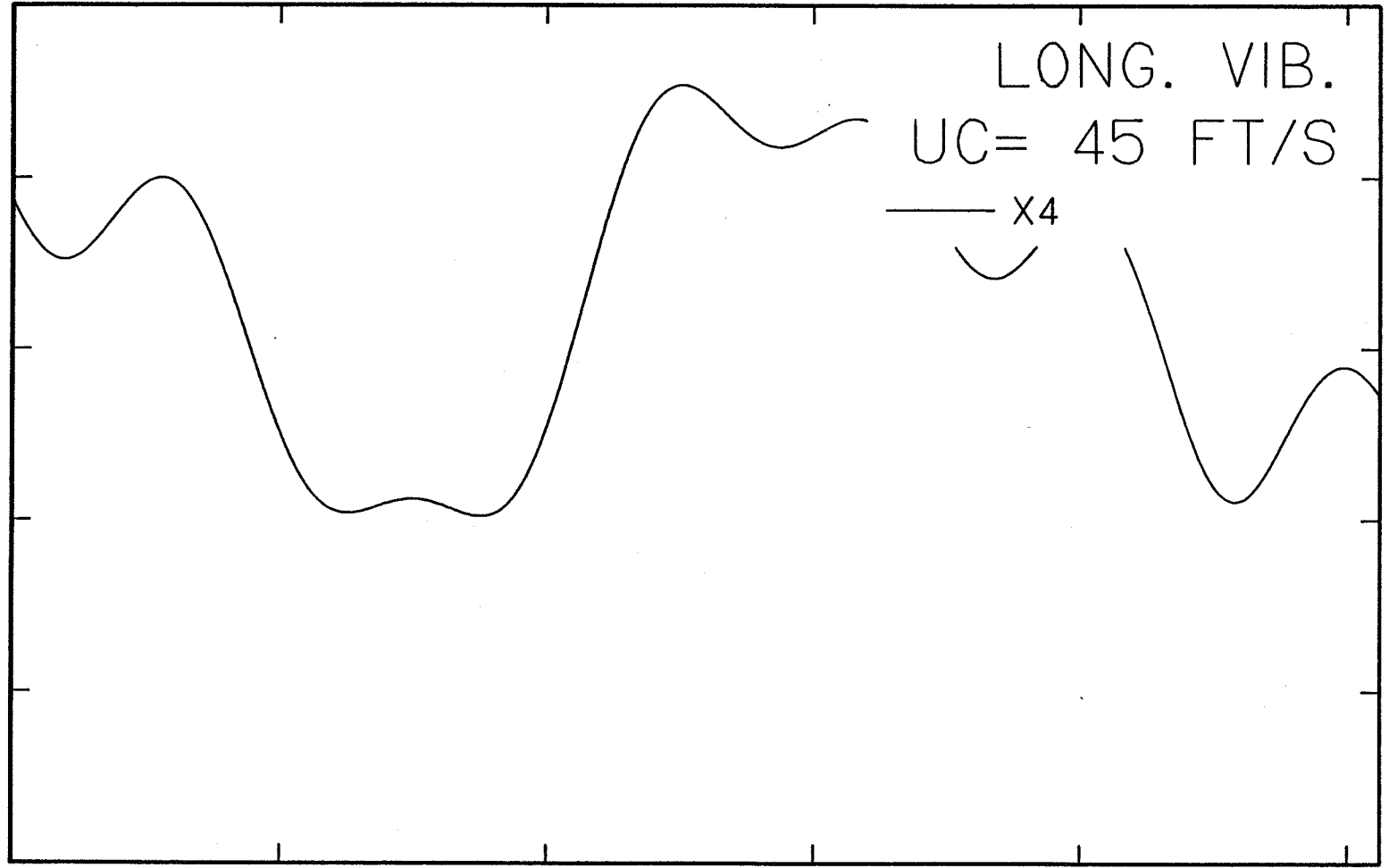
0.020

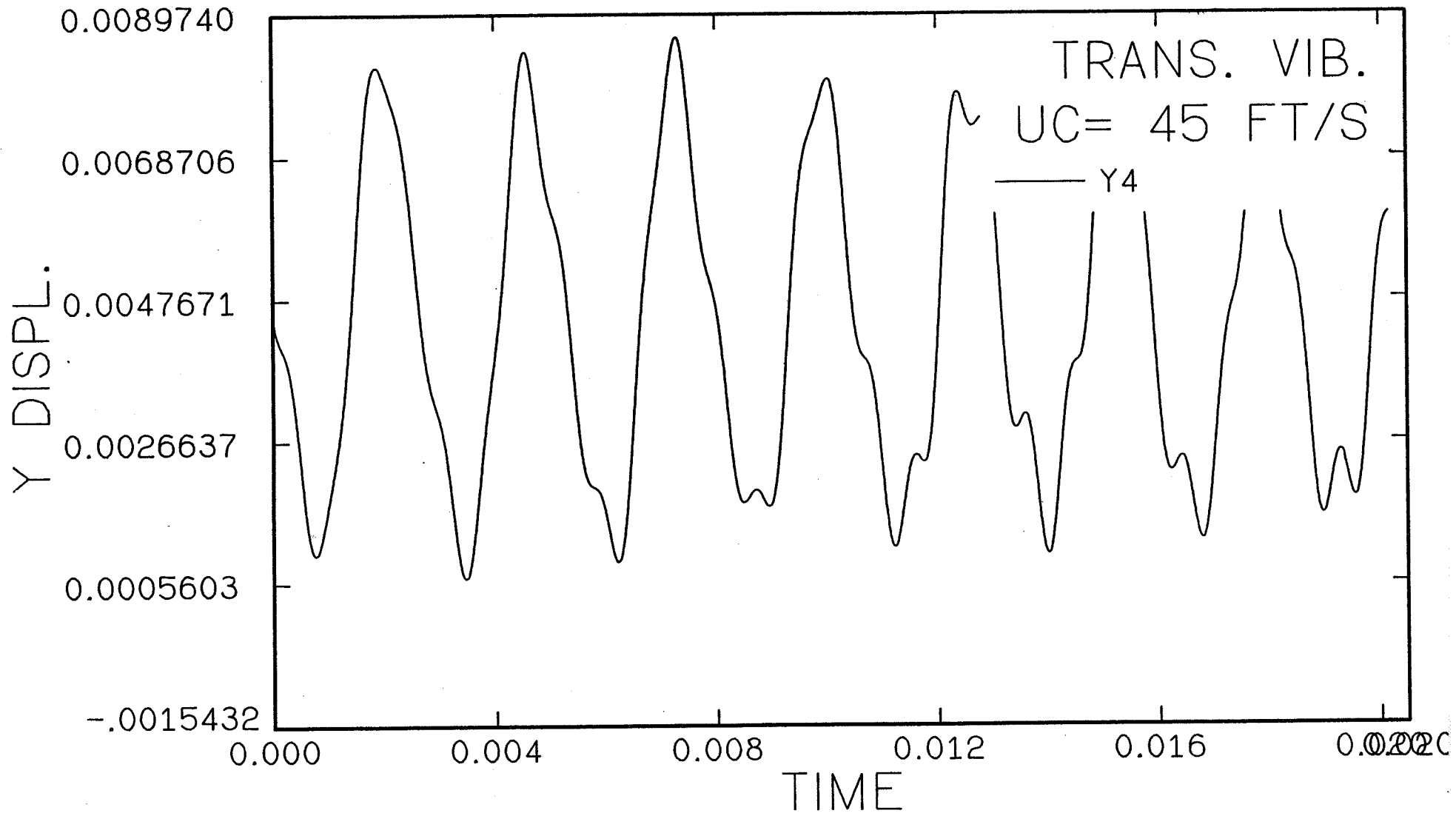
TIME

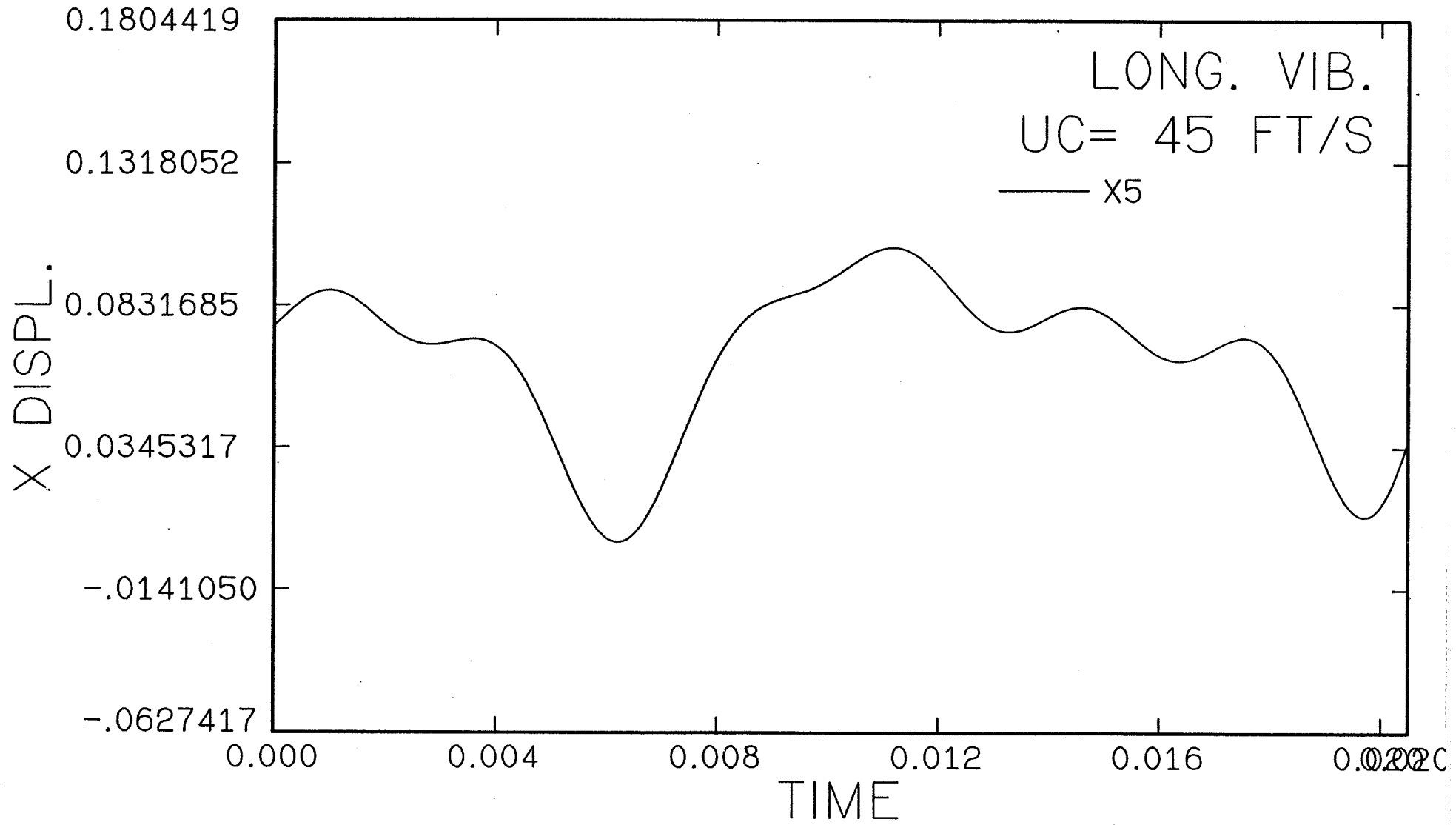
LONG. VIB.

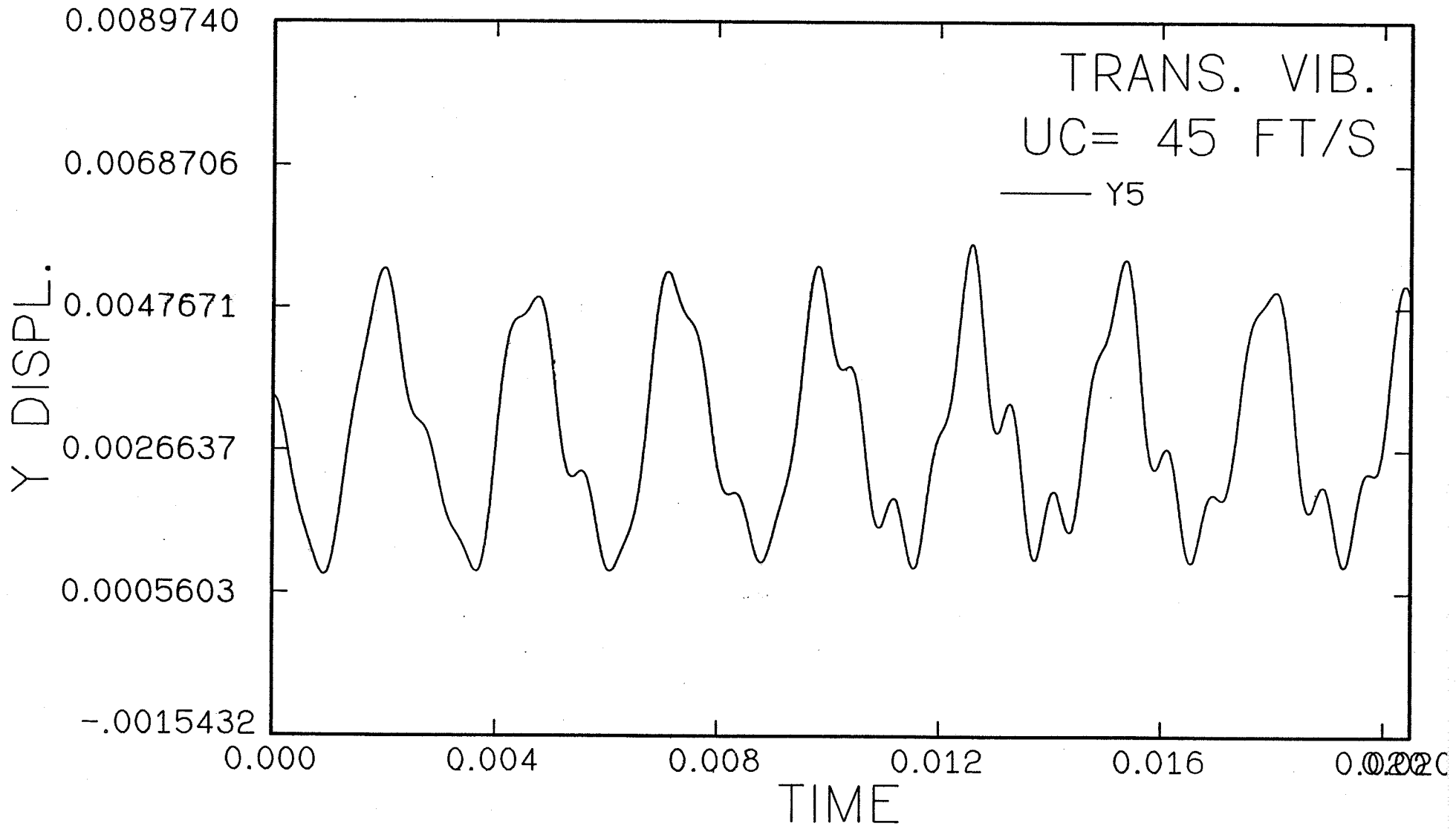
UC= 45 FT/S

x4

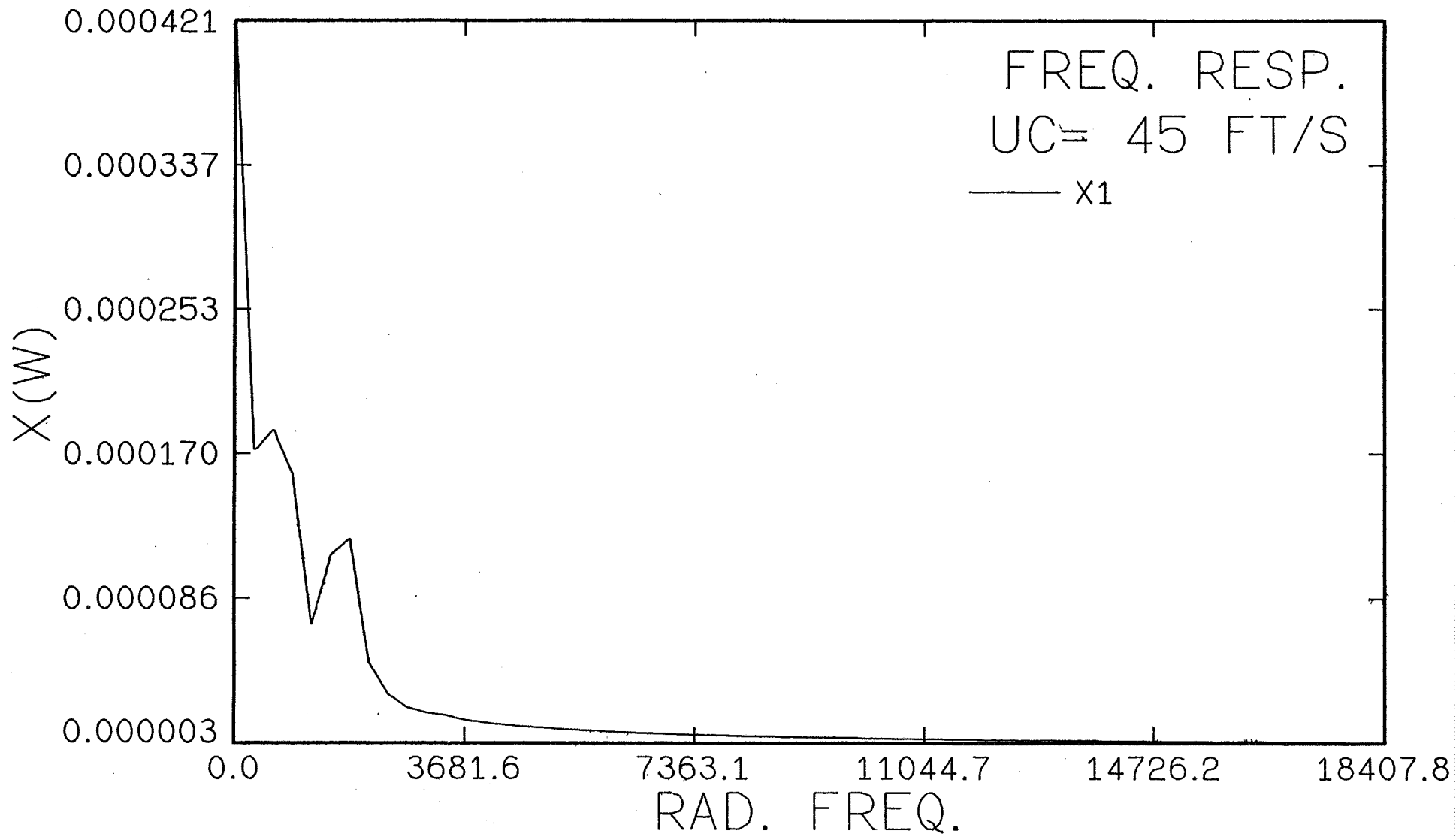


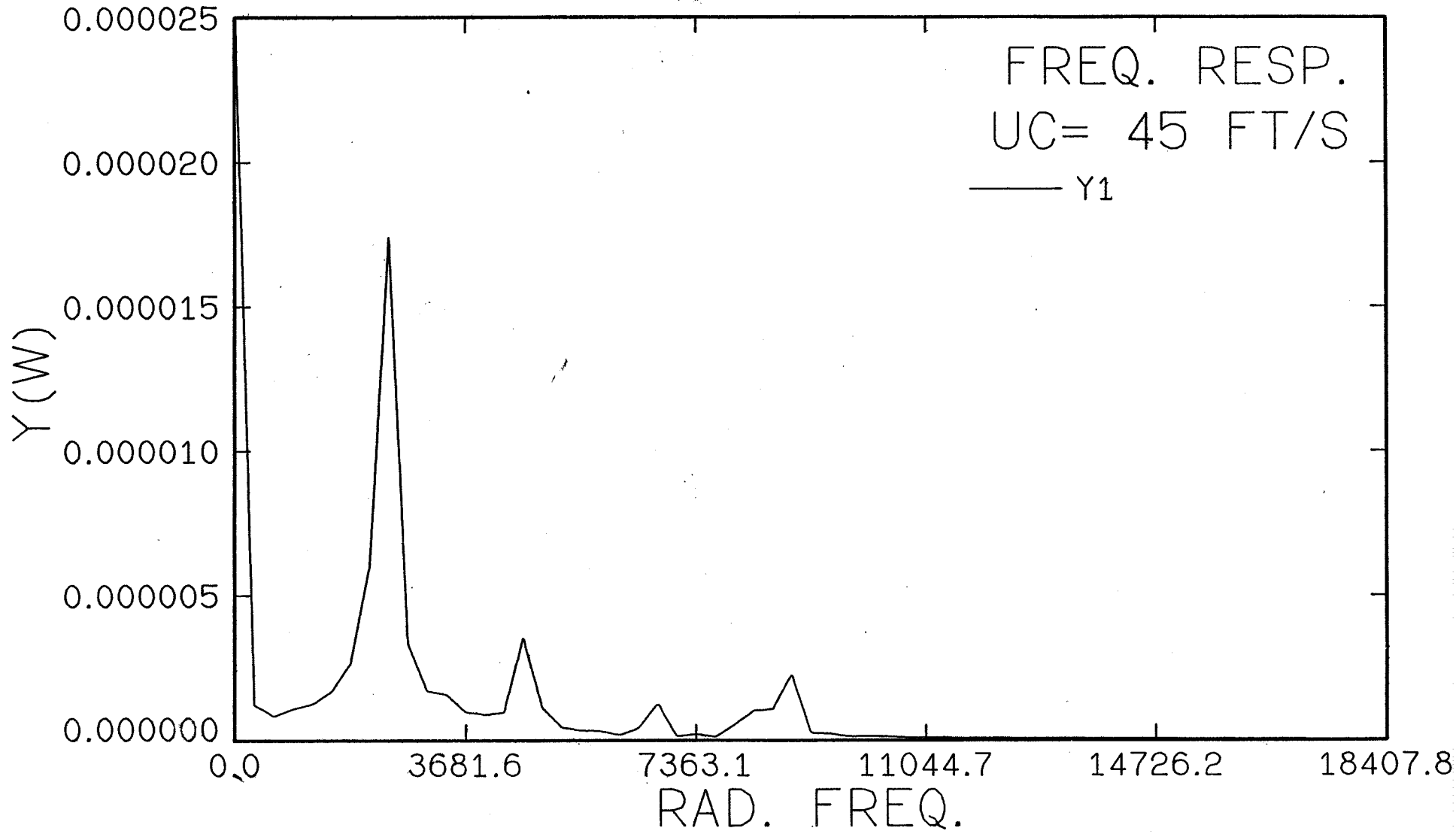


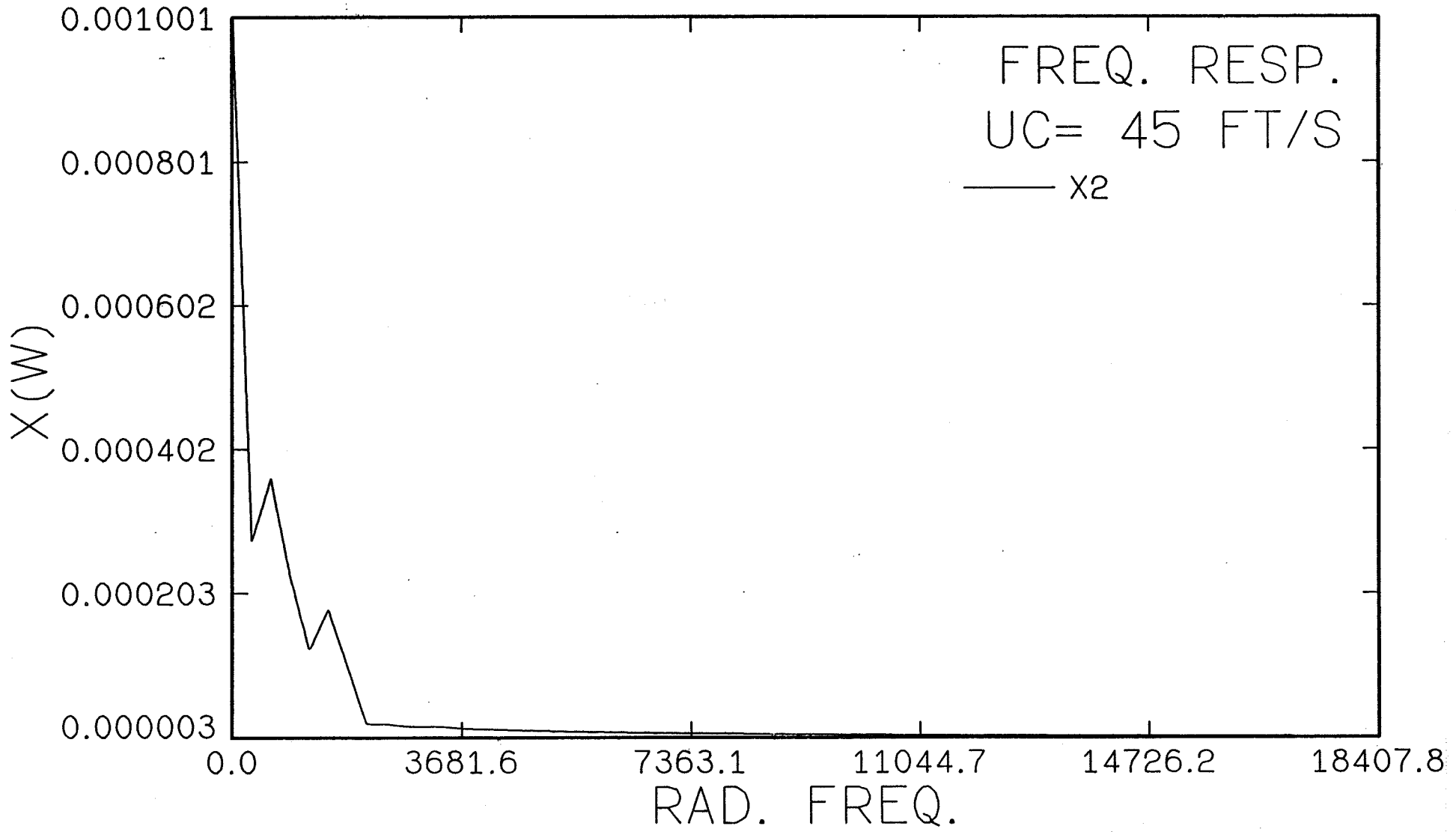


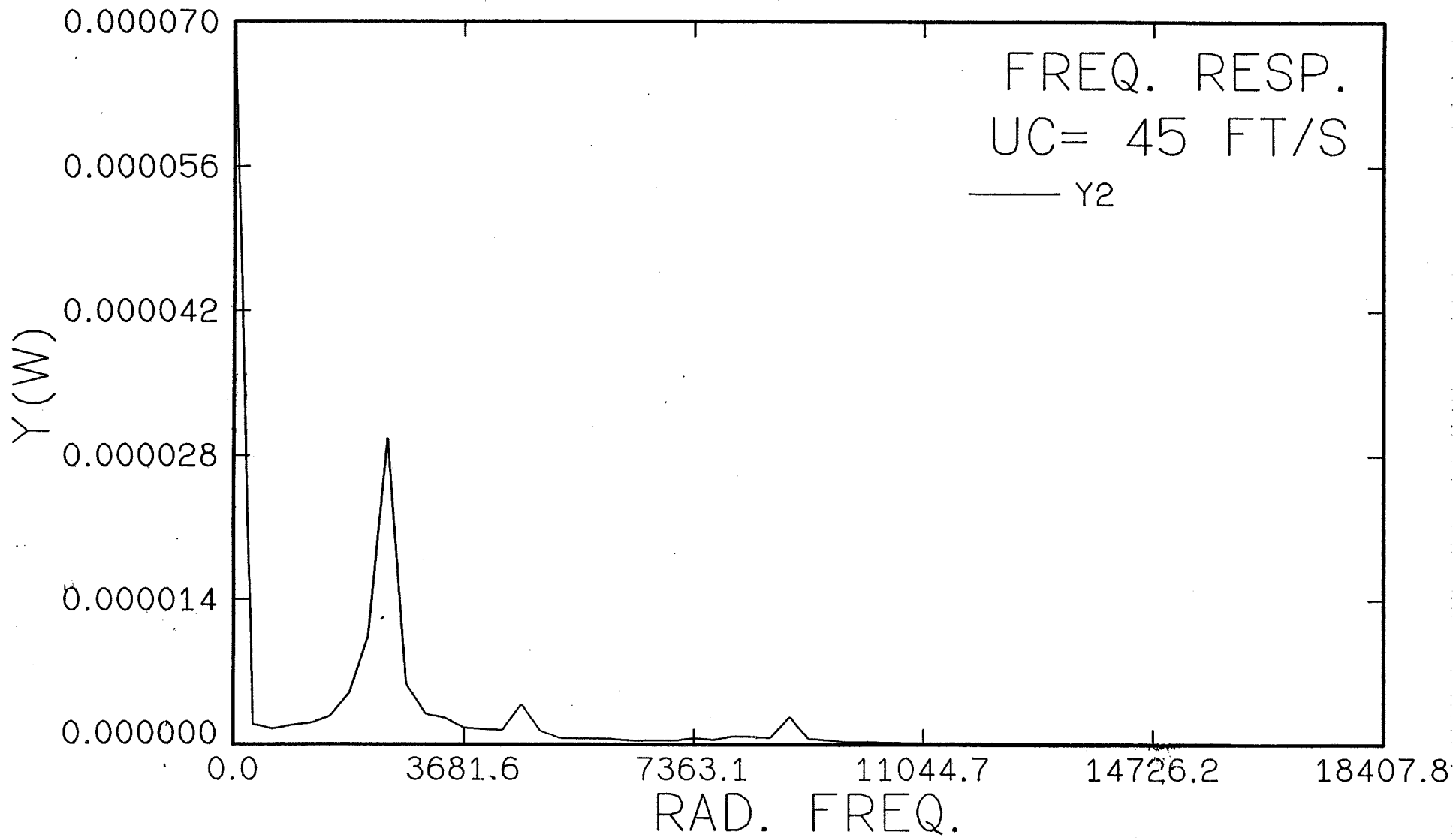


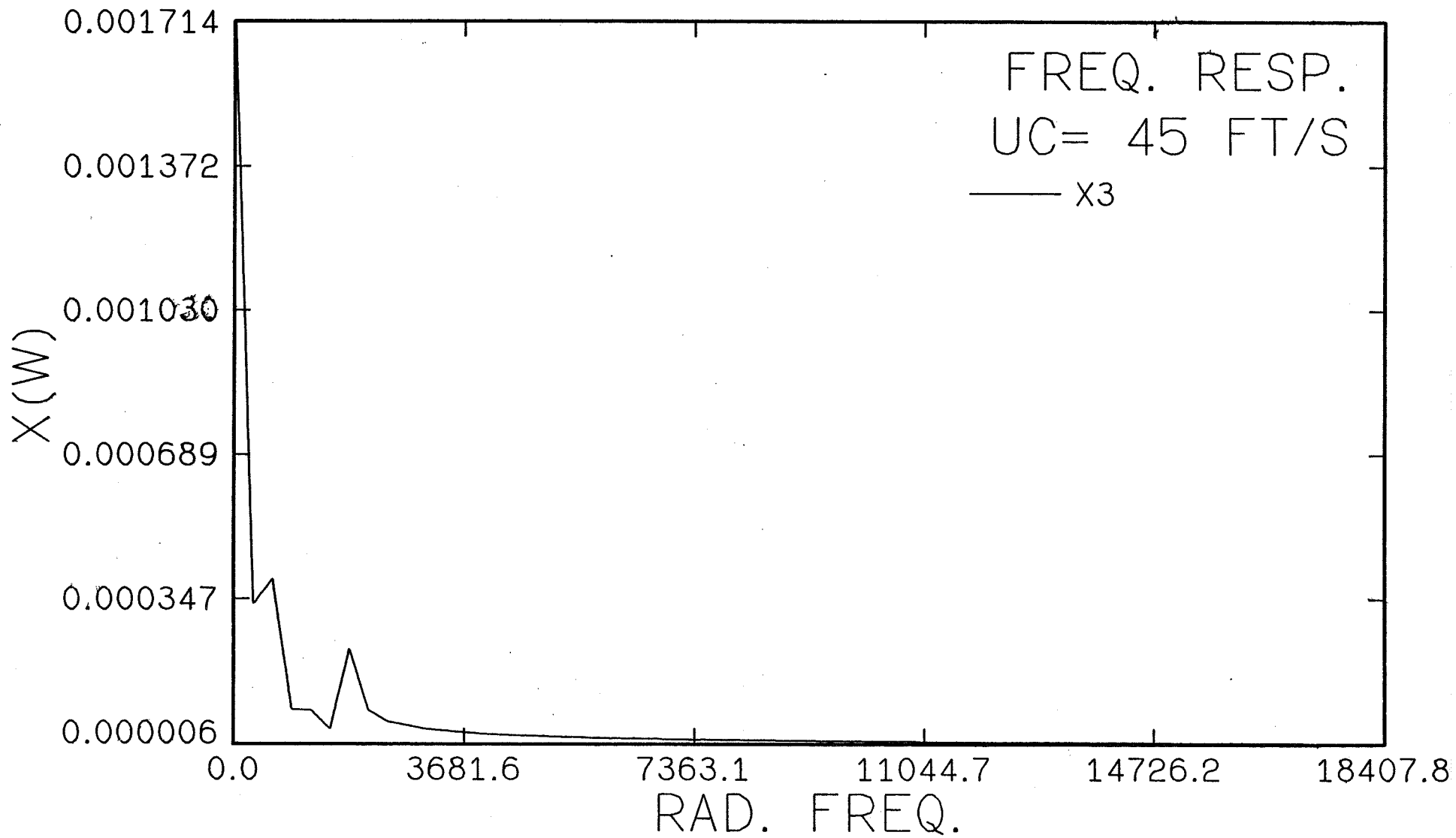
- 55 -



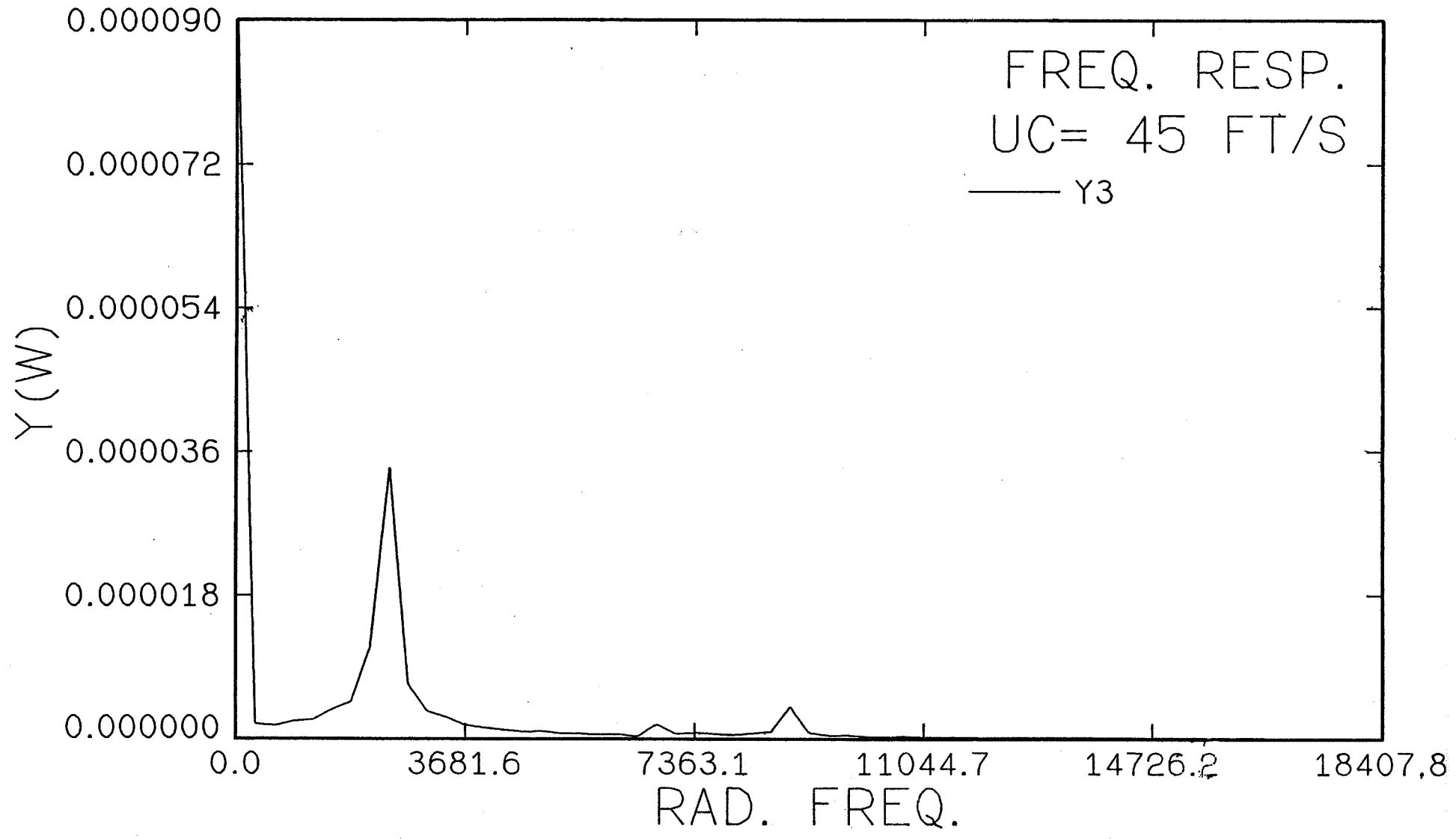




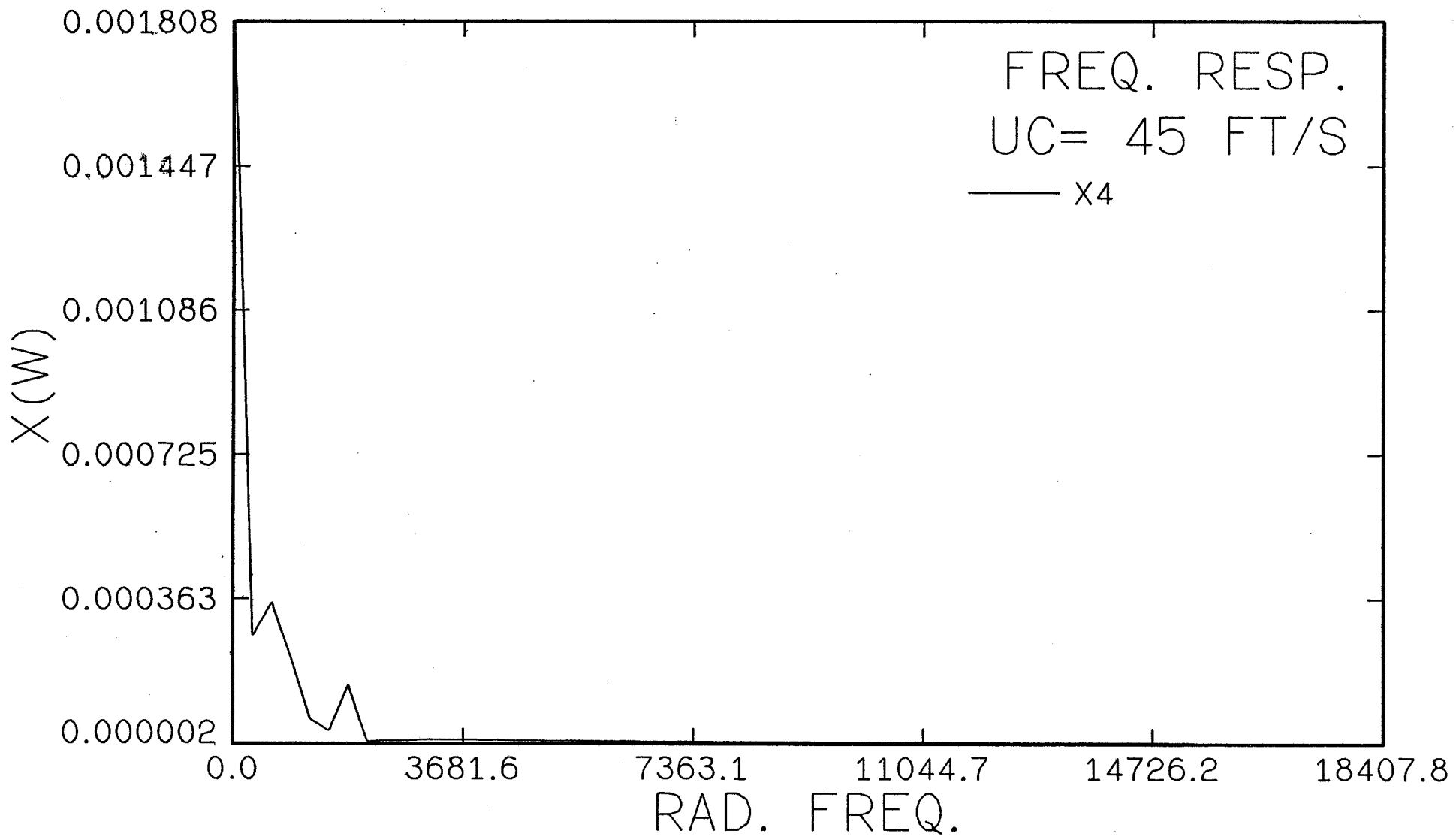


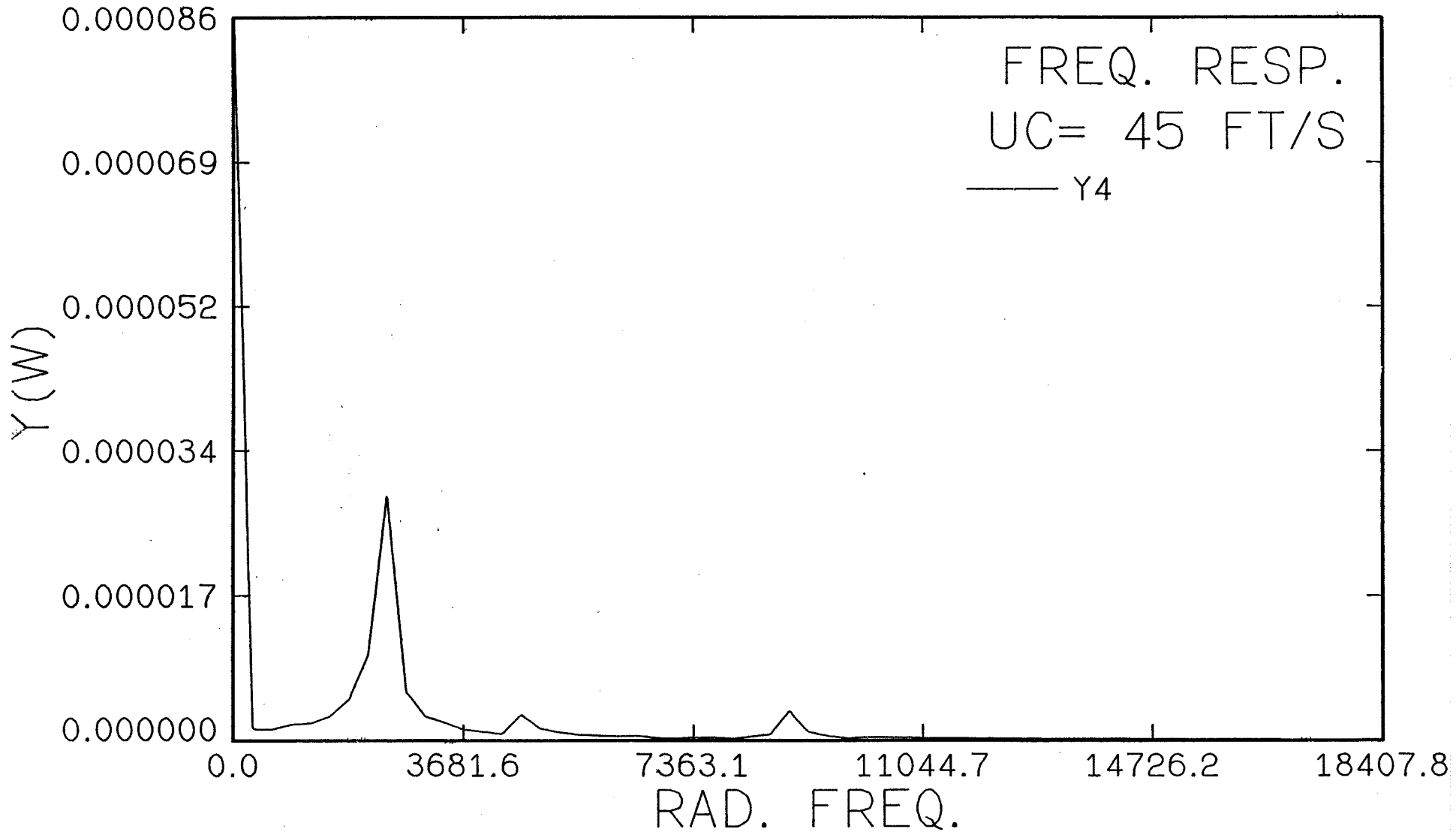


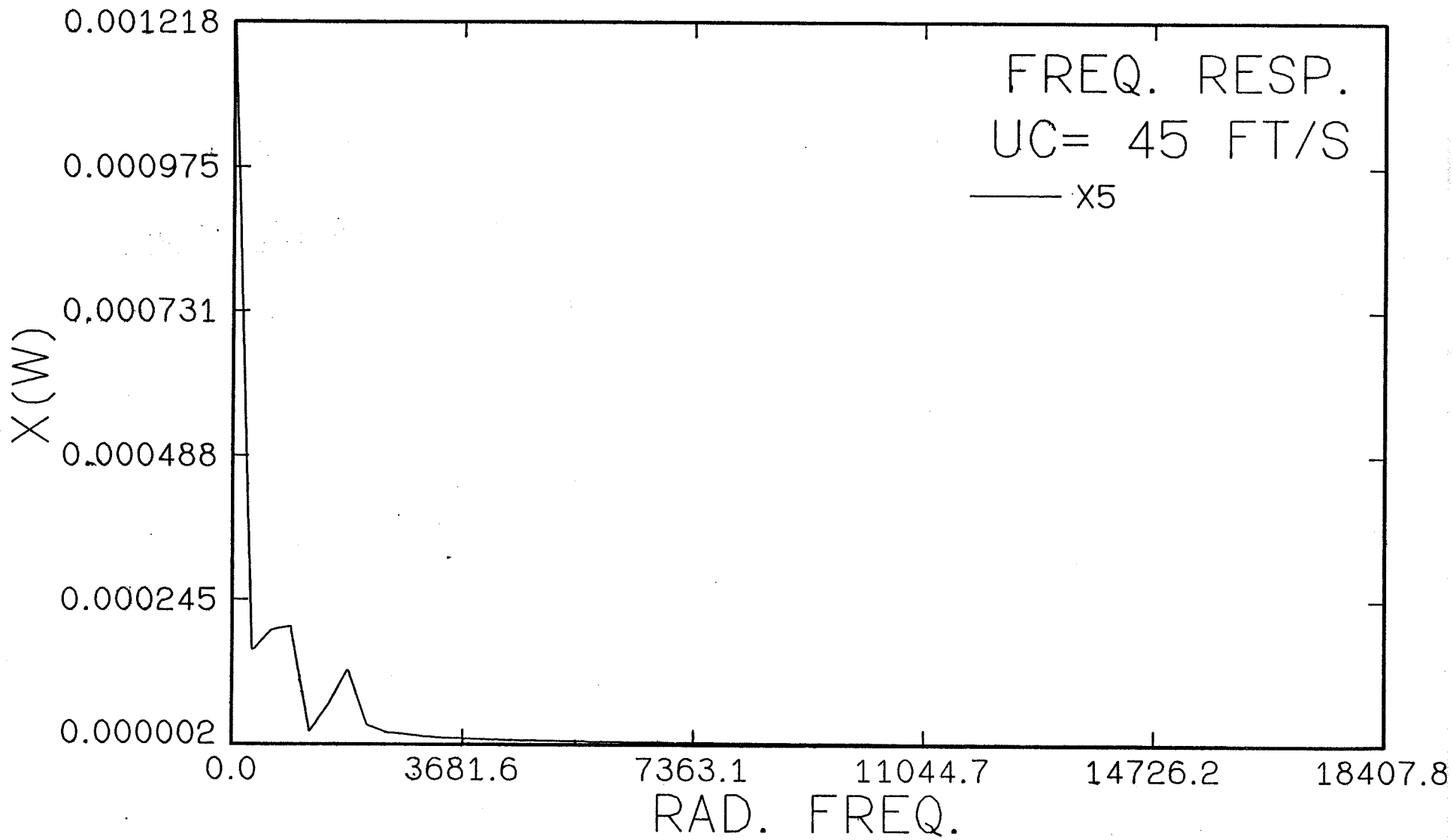
- 09 -

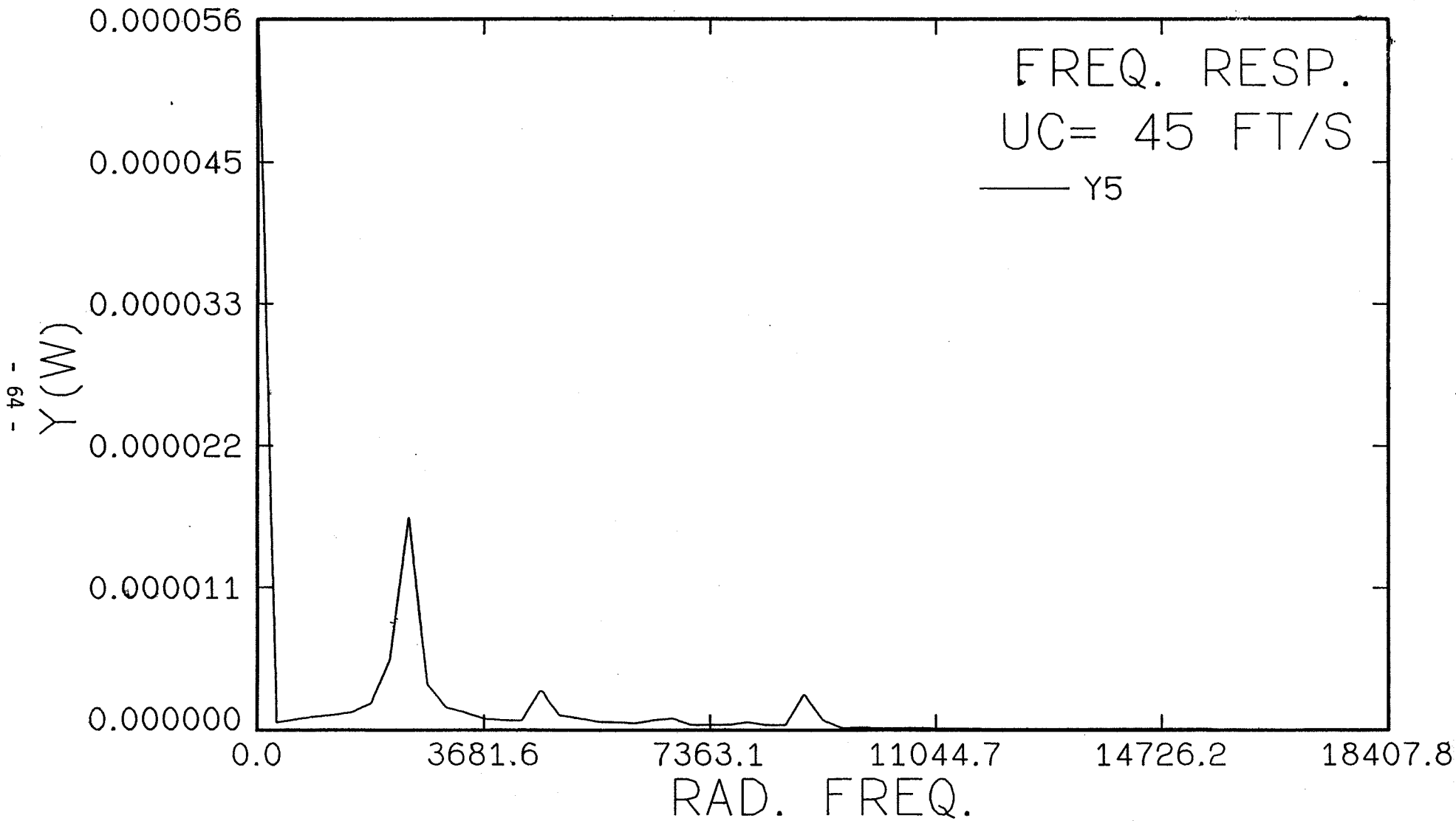


- 19 -









APPENDIX II

LISTING OF PROGRAM BELLOWS

PROGRAM BELLOWS (INPUT,OUTPUT,TAPE5=INPUT,TAPE6=OUTPUT)

```
C
C *****
C *
C *          BELLOWS FATIGUE PROGRAM          *
C *          1/28/86                          *
C *
C *
C *
C * INVESTIGATOR: DR. P. V. DESAI             *
C * ASSISTANT: L. D. THORNHILL                *
C *
```

```
C *****
C
C THIS PROGRAM COMPUTES AN ESTIMATE OF THE FATIGUE
C LIFE OF BELLOWS UNDER A VARIETY OF OPERATIONAL
C CONDITIONS.
```

```
C
C     CALL ENTER
C     CALL RUNGE
C     CALL HAMM
C     CALL STRAIN
C     CALL FFT
C     CALL CYCLE
C     CALL DAMAGE
C     CALL RESULT
```

```
C
C     STOP
C     END
```

```
C
C     SUBROUTINE ENTER
```

```
C
C ENTER GEOMETRIC, MATERIAL AND FLOW PARAMETERS AND
C CALCULATE EQUATION CONSTANTS.
```

```
C
C     COMMON/BLOK1/ PI,DELO,PIDEN,ALO,TE,EM,UC,UCT,N
C     COMMON/BLOK2/ XK,YK,FDX,FDY,DENSA
C     COMMON/BLOK5/ A1,E,BOTX2,BOTY2
C     DIMENSION FDX(9),FDY(9)
```

```
C
C     PRINT*, 'ENTER CONVOLUTE PITCH IN INCHES.'
C     READ*, PITCH
C     PRINT*, 'ENTER CONVOLUTE HEIGHT IN INCHES.'
C     READ*, HI
C     PRINT*, 'ENTER PLY THICKNESS IN INCHES.'
C     READ*, TPLY
C     PRINT*, 'ENTER NUMBER OF PLYS.'
C     READ*, NPLY
C     PRINT*, 'ENTER INSIDE BELLOWS DIA. IN INCHES.'
C     READ*, DIN
C     PRINT*, 'ENTER NUMBER OF CONVOLUTES.'
C     READ*, N
C     PRINT*, 'ENTER FLUID DENSITY IN LBM/(IN**3).'
C     READ*, DENF
C     PRINT*, 'ENTER FLOW VELOCITY IN FT/S.'
C     READ*,UFEET
C     PRINT*, 'ENTER THE ELASTIC MODULUS IN PSI.'
C     READ*, E1
```

```
PRINT*, 'ENTER THE MATERIAL DENSITY IN LBM/(IN**3).'  
READ*, DENM
```

C

```
TE=TPLY*FLOAT(NPLY)  
UC=UFEET*12.  
E=E1*12.  
G=E/(2.*(1.+1./3.))
```

C

```
PRINT*, 'CONVOLUTE PITCH IS ',PITCH,' IN.'  
PRINT*, 'CONVOLUTE HEIGHT IS ',HI,' IN.'  
PRINT*, 'PLY THICKNESS IS ',TPLY,' IN.'  
PRINT*, 'NUMBER OF PLYS IS ',NPLY  
PRINT*, 'INSIDE BELLOWS DIA. IS ',DIN,' IN.'  
PRINT*, 'NUMBER OF CONVOLUTES IS ',N  
PRINT*, 'FLUID DENSITY IS ',DENF,' LBM/(IN**3)'  
PRINT*, 'FLOW VELOCITY IS ',UFEET,' FT/S'  
PRINT*, 'ELASTIC MODULUS IS ',E1,' PSI'  
PRINT*, 'MATERIAL DENSITY IS ',DENM,' LBM/(IN**3)'
```

C

```
DO 3 J=1,N  
  FDX(J)=8.  
  FDY(J)=2.
```

3

```
CONTINUE
```

C

C CALCULATE EQUATION CONSTANTS

C

```
IF (UC .GT. 0. .AND. UC .LE. 180.) ALPHA=1.3  
IF (UC .GT. 180. .AND. UC .LE. 300.) ALPHA=1.2  
IF (UC .GT. 300. .AND. UC .LE. 420.) ALPHA=1.0  
IF (UC .GT. 420. .AND. UC .LE. 540.) ALPHA=0.6  
IF (UC .GT. 540. .AND. UC .LE. 660.) ALPHA=0.4  
IF (UC .GT. 660. .AND. UC .LE. 780.) ALPHA=0.1  
IF (UC .GT. 780.) ALPHA=0.05  
R= PITCH/4.  
PI= 4.*ATAN(1.)  
DOUT=DIN+2.*HI+2.*TE  
DM= (DIN+DOUT)/2.  
SIGMA= (2.*R)+TE  
DELO= (2.*R)-TE  
ALO= HI-(2.*R)  
PIDEN= PI*DM*DENF  
EM= PI*DM*DENM*(R*((2.*PI)-4.)+2.*HI)*TE
```

C

```
AMOM1= (PI*DIN*(TE**3.))/12.  
AMOM2= (PI*DM*(TE**3.))/12.  
AMOM3= (PI*DOUT*(TE**3.))/12.
```

C

```
A1=PI*DIN*TE  
A2=PI*DM*TE  
A3=PI*DOUT*TE  
B=HI-2.*R
```

C

```
BOTTOM= (PI/32.)*((R**3.)/(E*AMOM1) + R/(E*A1)  
$ + R/(G*A1) + R/(E*A3) + R/(G*A3)) + 0.125*(((R**2.)/  
$ (E*AMOM2))*B + B/(E*A2)) + ((9.*PI-16.)/32.)*((R**3.)/  
$ (E*AMOM3))  
BOTY2=(PI/32.)*((R**3.)/(E*AMOM1)+R/(E*A1)+R/(G*A1))
```

C

```
YK= 1./BOTTOM
```

C

C1=(3.*PI)/8.-1.
 C2=PI/8.
 C3=1.+(3.*PI)/8.
 C4=1.+PI/2.
 C5=PI/4.

C

BOTX=C1*(R**3.)/(E*AMOM1)+(C2*R*(A1+A3)*(E+G))/(A1*A3*E*G)
 \$ +((R**2.)*B)/(2.*E*AMOM2)+B/(2.*G*A2)+C3*(R**3.)/(E
 \$ *AMOM3)+(C4*(R**2.)*B)/(E*AMOM3)+(C5*R*(B**2.))/(E
 \$ *AMOM3)
 BOTX2=BOTX-C3*(R**3.)/(E*AMOM3)-C4*(R**2.)*B/(E*AMOM3)
 \$ -C5*R*(B**2.)/(E*AMOM3)-C2*R/(E*A3)-C2*R/(G*A3)

C

XK=1./BOTX

A=(R+TE/2.)*(PI**2.)*DIN
 DENSA= 0.5*DENF*A
 UCT= UC*TAN(ALPHA)

C

RETURN
 END

C

C

C

SUBROUTINE RUNGE

C

C

C

CALCULATE STARTING VALUES FOR HAMMINGS METHOD.

C

COMMON/BLOK1/ PI,DELO,PIDEN,ALO,TE,EM,UC,UCT,N
 COMMON/BLOK3/ X,Y
 COMMON/BLOK35/ XP,XP1,XP2,XP3,XP4,YP,YP1,YP2,YP3,YP4,
 \$ XPP,XPP1,XPP2,XPP3,XPP4,YPP,YPP1,YPP2,YPP3,YPP4,
 \$ CD,CL
 DIMENSION X(0:6,0:2048),Y(0:6,0:2048),XP(0:6),XP1(0:6),
 \$ XP2(0:6),XP3(0:6),XP4(0:6),YP(0:6),YP1(0:6),
 \$ YP2(0:6),YP3(0:6),YP4(0:6),XPP(0:6),XPP1(0:6),
 \$ XPP2(0:6),XPP3(0:6),XPP4(0:6),YPP(0:6),YPP1(0:6),
 \$ YPP2(0:6),YPP3(0:6),YPP4(0:6),CD(5),CL(5)
 COMMON/BLOK4/ TX,TXP,TY,TYP,K,Q,H,L,J,I
 REAL K
 DIMENSION TX(3),TXP(3),TY(3),TYP(3),K(4),Q(4)

C

C

C

TIME STEP, H, AND CONSTANTS.

H= 0.00001
 A1= H/6.
 A2= 1./6.
 A3= H/2.
 A4= H/4.

C

C

C

INITIAL CONDITIONS

DO 10, J=0,N+1
 X(J,0)=0.0
 Y(J,0)=0.0
 XP(J)=0.0
 XP1(J)=0.0
 XP2(J)=0.0
 XP3(J)=0.0
 XP4(J)=0.0

```

    YP(J)=0.0
    YP1(J)=0.0
    YP2(J)=0.0
    YP3(J)=0.0
    YP4(J)=0.0
    XPP1(J)=0.0
    XPP2(J)=0.0
    XPP3(J)=0.0
    XPP4(J)=0.0
    YPP1(J)=0.0
    YPP2(J)=0.0
    YPP3(J)=0.0
    YPP4(J)=0.0
10  CONTINUE
C
C  BOUNDARY CONDITIONS
C
    DO 30, J=0,N+1,N+1
    DO 20, I=0,2048
        X(J,I)=0.0
        Y(J,I)=0.0
20  CONTINUE
30  CONTINUE
C
C  RUNGE KUTTA STARTER.
C
    DO 50, I=0,3
C
    DO 31, J=1,N
        XP4(J)=XP3(J)
        XP3(J)=XP2(J)
        XP2(J)=XP1(J)
        XP1(J)=XP(J)
        YP4(J)=YP3(J)
        YP3(J)=YP2(J)
        YP2(J)=YP1(J)
        YP1(J)=YP(J)
        XPP4(J)=XPP3(J)
        XPP3(J)=XPP2(J)
        XPP2(J)=XPP1(J)
        YPP4(J)=YPP3(J)
        YPP3(J)=YPP2(J)
        YPP2(J)=YPP1(J)
31  CONTINUE
C
    DO 40, J=1,N
C
    DO 32, M=1,3
        IND= J+(2-M)
        TX(M)=X(IND,I)
        TXP(M)=XP1(IND)
        TY(M)=Y(IND,I)
        TYP(M)=YP1(IND)
32  CONTINUE
C
        L=1
        CALL KQ
C
    DO 34, M=1,3
        IND=J+(2-M)

```

$TX(M) = X(IND, I) + A3 * XP1(IND)$
 $TXP(M) = XP1(IND) + (K(1) / 2.)$
 $TY(M) = Y(IND, I) + A3 * YP1(IND)$
 $TYP(M) = YP1(IND) + (Q(1) / 2.)$

34 CONTINUE

C

L=2
CALL KQ

C

DO 36, M=1,3
IND=J+(2-M)
 $TX(M) = X(IND, I) + A3 * XP1(IND) + A4 * K(1)$
 $TXP(M) = XP1(IND) + (K(2) / 2.)$
 $TY(M) = Y(IND, I) + A3 * YP1(IND) + A4 * Q(1)$
 $TYP(M) = YP1(IND) + (Q(2) / 2.)$

36 CONTINUE

C

L=3
CALL KQ

C

DO 38, M=1,3
IND=J+(2-M)
 $TX(M) = X(IND, I) + H * XP1(IND) + A3 * K(2)$
 $TXP(M) = XP1(IND) + K(3)$
 $TY(M) = Y(IND, I) + H * YP1(IND) + A3 * Q(2)$
 $TYP(M) = YP1(IND) + Q(3)$

38 CONTINUE

C

L=4
CALL KQ

C

$X(J, I+1) = X(J, I) + H * XP1(J) + A1 * (K(1) + K(2) + K(3))$
 $XP(J) = XP1(J) + A2 * (K(1) + 2. * K(2) + 2. * K(3) + K(4))$
 $Y(J, I+1) = Y(J, I) + H * YP1(J) + A1 * (Q(1) + Q(2) + Q(3))$
 $YP(J) = YP1(J) + A2 * (Q(1) + 2. * Q(2) + 2. * Q(3) + Q(4))$

C

40 CONTINUE

50 CONTINUE

C

RETURN
END

C

C

C

C

SUBROUTINE KQ

COMMON/BLOK1/ PI, DELO, PIDEN, ALO, TE, EM, UC, UCT, N
COMMON/BLOK2/ XK, YK, FDX, FDY, DENSA
DIMENSION FDX(9), FDY(9)
COMMON/BLOK3/ X, Y
COMMON/BLOK35/ XP, XP1, XP2, XP3, XP4, YP, YP1, YP2, YP3, YP4,
\$ XPP, XPP1, XPP2, XPP3, XPP4, YPP, YPP1, YPP2, YPP3, YPP4,
\$ CD, CL
DIMENSION X(0:6, 0:2048), Y(0:6, 0:2048), XP(0:6), XP1(0:6),
\$ XP2(0:6), XP3(0:6), XP4(0:6), YP(0:6), YP1(0:6),
\$ YP2(0:6), YP3(0:6), YP4(0:6), XPP(0:6), XPP1(0:6),
\$ XPP2(0:6), XPP3(0:6), XPP4(0:6), YPP(0:6), YPP1(0:6),
\$ YPP2(0:6), YPP3(0:6), YPP4(0:6), CD(5), CL(5)
COMMON/BLOK4/ TX, TXP, TY, TYP, K, Q, H, L, J, I
REAL K

DIMENSION TX(3),TXP(3),TY(3),TYP(3),K(4),Q(4)

C

DIFF=DELO+TX(2)-TX(3)

XMAS= PIDEN*((PI/8.)*(DIFF**2.))+DIFF*(ALO+0.5*DELO+TE
\$ +0.5*(1.-PI)*(TX(2)-TX(3)))+0.5*(4.-PI)*((0.5*DIFF
\$ +TE)**2.))+EM

YMAS=XMAS

C

CD(1)=-0.5

CL(1)=0.2

DO 10 KOUNT=2,N

CD(KOUNT)=0.085

CL(KOUNT)=0.08

10 CONTINUE

C

TERM1=UCT+TYP(2)-TYP(3)

TERM2=UC+TXP(2)-TXP(3)

C

XPP1(J)=FCN1(XMAS,TERM1,TERM2, TX(1),TX(2),TX(3),TXP(1),
\$ TXP(2),TXP(3),TYP(2),TYP(3),CD(J),CL(J),FDX(J),FDY(J))
K(L)=H*XPP1(J)

C

YPP1(J)=FCN2(YMAS,TERM1,TERM2, TY(1),TY(2),TY(3),TYP(1),
\$ TYP(2),TYP(3),TXP(2),TXP(3),CD(J),CL(J),FDX(J),FDY(J))
Q(L)=H*YPP1(J)

C

RETURN

END

C

C

C

FUNCTION FCN1(XMAS,TERM1,TERM2,X1,X2,X3,VX1,VX2,VX3,VY2,
\$ VY3,CD,CL,DX,DY)
COMMON/BLOK2/ XK,YK,FDX,FDY,DENSA
DIMENSION FDX(9),FDY(9)

C

FCN1=(DENSA*(SQRT((TERM1**2.)+(TERM2**2.)))*(CL*TERM1
\$ +CD*TERM2)+DX*SIGN(1.,VX2)+XK*(X1-2.*X2+X3))/XMAS

C

RETURN

END

C

C

C

FUNCTION FCN2(YMAS,TERM1,TERM2,Y1,Y2,Y3,VY1,VY2,VY3,VX2,
\$ VX3,CD,CL,DX,DY)
COMMON/BLOK2/ XK,YK,FDX,FDY,DENSA
DIMENSION FDX(9),FDY(9)

C

FCN2=(DENSA*(SQRT((TERM1**2.)+(TERM2**2.)))*(CL*TERM2
\$ +CD*TERM1)+DY*SIGN(1.,VY2)+YK*(Y1-2.*Y2+Y3))/YMAS

C

RETURN

END

C

C

C

SUBROUTINE HAMM

C

C IMPLEMENTING HAMMINGS METHOD FOR SOLVING GOVERNING EQUATIONS.

C

```
COMMON/BLOK1/ PI,DELO,PIDEN,ALO,TE,EM,UC,UCT,N
COMMON/BLOK2/ XK,YK,FDX,FDY,DENSA
DIMENSION FDX(9),FDY(9)
COMMON/BLOK3/ X,Y
COMMON/BLOK35/ XP,XP1,XP2,XP3,XP4,YP,YP1,YP2,YP3,YP4,
$      XPP,XPP1,XPP2,XPP3,XPP4,YPP,YPP1,YPP2,YPP3,YPP4,
$      CD,CL
DIMENSION X(0:6,0:2048),Y(0:6,0:2048),XP(0:6),XP1(0:6),
$      XP2(0:6),XP3(0:6),XP4(0:6),YP(0:6),YP1(0:6),
$      YP2(0:6),YP3(0:6),YP4(0:6),XPP(0:6),XPP1(0:6),
$      XPP2(0:6),XPP3(0:6),XPP4(0:6),YPP(0:6),YPP1(0:6),
$      YPP2(0:6),YPP3(0:6),YPP4(0:6),CD(5),CL(5)
DIMENSION PX(0:6),PX1(0:6),PXP(0:6),PXP1(0:6),PY(0:6),
$      PY1(0:6),PYP(0:6),PYP1(0:6),CX(0:6),CX1(0:6),CXP(0:6),
$      CXP1(0:6),CY(0:6),CY1(0:6),CYP(0:6),CYP1(0:6),MX(0:6),
$      MXP(0:6),MY(0:6),MYP(0:6)
REAL MX,MXP,MY,MYP
```

C

C TIME STEP, H, AND EQUATION CONSTANTS.

C

```
H=0.00001
A=(4.*H)/3.
B=112./121.
C=1./8.
D=3.*H
AB=9./121.
```

C

C INITIAL VALUE LOOP.

C

```
DO 3, J=0,N+1
  I=3
  PX(J)=X(J,I)
  CX(J)=X(J,I)
  PXP(J)=XP1(J)
  CXP(J)=XP1(J)
  PY(J)=Y(J,I)
  CY(J)=Y(J,I)
  PYP(J)=YP1(J)
  CYP(J)=YP1(J)
```

3 CONTINUE

C

C BOUNDARY VALUE LOOP.

C

```
DO 9, J=0,N+1,N+1
  MX(J)=0.0
  MXP(J)=0.0
  MY(J)=0.0
  MYP(J)=0.0
```

9 CONTINUE

C

C *** HAMMINGS METHOD ***

C

```
DO 60, K=1,2
```

C

C REESTABLISH INITIAL CONDITIONS.

C

```
IF (K .EQ. 1) GO TO 14
DO 12, I=0,3
  IND=2048-3+I
```

```

DO 10, J=0,N+1
  X(J,I)=X(J,IND)
  Y(J,I)=Y(J,IND)
10 CONTINUE
12 CONTINUE
C
14 DO 50, I=3,2047
  DO 20, J=1,N
C
C PREDICTOR
C
  PXP1(J)=XP4(J)+A*(2.*XPP1(J)-XPP2(J)+2.*XPP3(J))
  PX1(J)=X(J,I-3)+A*(2.*XP1(J)-XP2(J)+2.*XP3(J))
  PYP1(J)=YP4(J)+A*(2.*YPP1(J)-YPP2(J)+2.*YPP3(J))
  PY1(J)=Y(J,I-3)+A*(2.*YP1(J)-YP2(J)+2.*YP3(J))
C
C MODIFIER
C
  MXP(J)=PXP1(J)-B*(PXP(J)-CXP(J))
  MX(J)=PX1(J)-B*(PX(J)-CX(J))
  MYP(J)=PYP1(J)-B*(PYP(J)-CYP(J))
  MY(J)=PY1(J)-B*(PY(J)-CY(J))
20 CONTINUE
C
C FUNCTION EVALUATIONS
C
  DO 30, J=1,N
  DIFF=DELO+MX(J)-MX(J-1)
  XMAS=PIDEN*((PI/8.)*(DIFF**2.))+DIFF*(ALO+0.5*DELO+0.5*(1.
$   -PI)*(MX(J)-MX(J-1)))+0.5*(4.-PI)*((0.5*DIFF
$   +TE)**2.))+EM
  YMAS=XMAS
  TERM1=UCT+MYP(J)-MYP(J-1)
  TERM2=UC+MXP(J)-MXP(J-1)
C
  XPP(J)=(DENSEA*(SQRT((TERM1**2.)+(TERM2**2.)))*CL(J)
$   *TERM1+CD(J)*TERM2)+FDX(J)*SIGN(1.,MXP(J))
$   +XK*(MX(J+1)-2.*MX(J)+MX(J-1)))/
$   XMAS
C
  YPP(J)=(DENSEA*(SQRT((TERM1**2.)+(TERM2**2.)))*CL(J)
$   *TERM2+CD(J)*TERM1)+FDY(J)*SIGN(1.,MYP(J))
$   +YK*(MY(J+1)-2.*MY(J)+MY(J-1)))/
$   YMAS
30 CONTINUE
C
  DO 40, J=1,N
C
C CORRECTOR
C
  CXP1(J)=C*(9.*XP1(J)-XP3(J)+D*(XPP(J)+2.*XPP1(J)
$   -XPP2(J)))
  CX1(J)=C*(9.*X(J,I)-X(J,I-2)+D*(CXP1(J)+2.*XP1(J)
$   -XP2(J)))
  CYP1(J)=C*(9.*YP1(J)-YP3(J)+D*(YPP(J)+2.*YPP1(J)
$   -YPP2(J)))
  CY1(J)=C*(9.*Y(J,I)-Y(J,I-2)+D*(CYP1(J)+2.*YP1(J)
$   -YP2(J)))
C
C FINAL VALUE

```

```

C
  XP(J)=CXP1(J)+AB*(PXP1(J)-CXP1(J))
  X(J,I+1)=CX1(J)+AB*(PX1(J)-CX1(J))
  YP(J)=CYP1(J)+AB*(PYP1(J)-CYP1(J))
  Y(J,I+1)=CY1(J)+AB*(PY1(J)-CY1(J))
40 CONTINUE
C
DO 45, J=0,N+1
  PX(J)=PX1(J)
  PXP(J)=PXP1(J)
  PY(J)=PY1(J)
  PYP(J)=PYP1(J)
  CX(J)=CX1(J)
  CXP(J)=CXP1(J)
  CY(J)=CY1(J)
  CYP(J)=CYP1(J)
  XP4(J)=XP3(J)
  XP3(J)=XP2(J)
  XP2(J)=XP1(J)
  XP1(J)=XP(J)
  YP4(J)=YP3(J)
  YP3(J)=YP2(J)
  YP2(J)=YP1(J)
  YP1(J)=YP(J)
  XPP4(J)=XPP3(J)
  XPP3(J)=XPP2(J)
  XPP2(J)=XPP1(J)
  XPP1(J)=XPP(J)
  YPP4(J)=YPP3(J)
  YPP3(J)=YPP2(J)
  YPP2(J)=YPP1(J)
  YPP1(J)=YPP(J)
45 CONTINUE
50 CONTINUE
60 CONTINUE
C
  RETURN
  END
C
C
C
  SUBROUTINE STRAIN
C
C THIS SUBROUTINE COMPUTES THE STRAIN AMPLITUDE FOR
C EACH OF THE CONVOLUTE TIPS.
C
  COMMON/BLOK1/ PI,DELO,PIDEN,ALO,TE,EM,UC,UCT,N
  COMMON/BLOK3/ X,Y
  COMMON/BLOK5/ A1,E,BOTX2,BOTY2
  COMMON/BLOK6/ SAMP
  DIMENSION X(0:6,0:2048),Y(0:6,0:2048),SAMP(5),
$           EXMAX(5),EXMIN(5),EYMAX(5),EYMIN(5),
$           SMAX(5),SMIN(5)
C
  IF (N .GT. 1) GO TO 2
  AMULT=0.1
  GO TO 4
2  AMULT=0.13+0.29*FLOAT(N-2)
4  BOTX2=AMULT*BOTX2
  BOTY2=AMULT*BOTY2

```

```
TERMX=E*A1*BOTX2
TERMY=E*A1*BOTY2
```

C

```
DO 10 J=1,N
  EXMAX(J)=X(J,0)/TERMX
  EXMIN(J)=EXMAX(J)
  EYMAX(J)=Y(J,0)/TERMY
  EYMIN(J)=EYMAX(J)
```

10 CONTINUE

C

```
DO 30 I=1,2048
DO 20 J=1,N
  EPX=X(J,I)/TERMX
  EPY=Y(J,I)/TERMY
  EXMAX(J)=AMAX1(EXMAX(J),EPX)
  EXMIN(J)=AMIN1(EXMIN(J),EPX)
  EYMAX(J)=AMAX1(EYMAX(J),EPY)
  EYMIN(J)=AMIN1(EYMIN(J),EPY)
```

20 CONTINUE

30 CONTINUE

C

```
DO 35 J=1,N
  SMAX(J)=EXMAX(J)+EYMAX(J)
  SMIN(J)=EXMIN(J)+EYMIN(J)
```

35 CONTINUE

C

```
DO 40 J=1,N
  SAMP(J)=(SMAX(J)-SMIN(J))/2.
```

40 CONTINUE

C

```
RETURN
END
```

C

C

C

SUBROUTINE FFT

C

```
C THIS SUBROUTINE TRANSFORMS THE SYSTEM RESPONSE
C PREDICTED BY THE MODEL INTO THE FREQUENCY DOMAIN
C SO THAT THE DOMINANT FREQUENCIES MAY BE DETERMINED.
```

C

```
COMMON/BLOK1/ PI,DELO,PIDEN,ALO,TE,EM,UC,UCT,N
COMMON/BLOK3/ X,Y
COMMON/BLOK7/ XMAG,YMAG,OMEG
DIMENSION X(0:6,0:2048),Y(0:6,0:2048),U(0:2048),
$ XMAG(0:2048),YMAG(0:2048),OMEG(0:2048)
COMPLEX POWER,U,SUMX,SUMY,TERMX,TERMY,XT,YT
```

C

```
NUM=2048
H=0.00001
T=H*NUM
```

C

```
DO 50 I=0,NUM
  OMEG(I)=(2.*PI*FLOAT(I))/T
```

50 CONTINUE

C

```
DO 1000 J=1,N
```

C

```
DO 100 I=0,1
  A=FLOAT(I)
```

```

        POWER=CMPLX(0., (-2.*PI*A)/FLOAT(NUM))
        U(I)=CEXP(POWER)
100    CONTINUE
C
        DO 200 I=2,NUM
            U(I)=U(I-1)*U(1)
200    CONTINUE
C
        DO 400 K=0,NUM-1
            SUMX=CMPLX(0.,0.)
            SUMY=CMPLX(0.,0.)
        DO 300 M=0,NUM-1
            TERMX=X(J,M)*U(MOD(M*K,NUM))
            TERMY=Y(J,M)*U(MOD(M*K,NUM))
            SUMX=SUMX+TERMX
            SUMY=SUMY+TERMY
300    CONTINUE
            XT=H*SUMX
            YT=H*SUMY
            XMAG(K)=CABS(XT)
            YMAG(K)=CABS(YT)
400    CONTINUE
C
C
        CALL FINDFRQ (J)
C
C
1000   CONTINUE
C
        RETURN
        END
C
C
C
        SUBROUTINE FINDFRQ (J)
C
C THIS SUBROUTINE SEARCHES THROUGH THE FREQUENCY RESPONSE
C DATA AND DETERMINES THE THREE MOST DOMINANT FREQUENCIES
C IN BOTH THE LONGITUDINAL AND TRANSVERSE DIRECTIONS.
C
        COMMON/BLOK1/ PI,DELO,PIDEN,ALO,TE,EM,UC,UCT,N
        COMMON/BLOK7/ XMAG,YMAG,OMEG
        COMMON/BLOK8/ XFRQ,YFRQ
        DIMENSION XFRQ(3,5),YFRQ(3,5),XMAG(0:2048),YMAG(0:2048),
$          OMEG(0:2048),PK(3)
C
        P=2.*PI
C
        DO 10 K=1,3
            XFRQ(K,J)=0.0
            YFRQ(K,J)=0.0
            PK(K)=0.0
10     CONTINUE
C
        DO 30 I=2,60
            IF (XMAG(I) .LT. XMAG(I-1)) GO TO 30
            IF (XMAG(I) .LT. XMAG(I+1)) GO TO 30
C
            IF (PK(1) .GT. XMAG(I)) GO TO 22
            PK(3)=PK(2)

```

```

PK(2)=PK(1)
PK(1)=XMAG(I)
XFRQ(3, J)=XFRQ(2, J)
XFRQ(2, J)=XFRQ(1, J)
XFRQ(1, J)=OMEG(I)
GO TO 30
C
22  IF (PK(2) .GT. XMAG(I)) GO TO 24
    PK(3)=PK(2)
    PK(2)=XMAG(I)
    XFRQ(3, J)=XFRQ(2, J)
    XFRQ(2, J)=OMEG(I)
    GO TO 30
C
24  IF (PK(3) .GT. XMAG(I)) GO TO 30
    PK(3)=XMAG(I)
    XFRQ(3, J)=OMEG(I)
30  CONTINUE
C
DO 35 K=1,3
    PK(K)=0.0
35  CONTINUE
C
DO 40 I=2,60
    IF (YMAG(I) .LT. YMAG(I-1)) GO TO 40
    IF (YMAG(I) .LT. YMAG(I+1)) GO TO 40
C
    IF (PK(1) .GT. YMAG(I)) GO TO 36
    PK(3)=PK(2)
    PK(2)=PK(1)
    PK(1)=YMAG(I)
    YFRQ(3, J)=YFRQ(2, J)
    YFRQ(2, J)=YFRQ(1, J)
    YFRQ(1, J)=OMEG(I)
    GO TO 40
C
36  IF (PK(2) .GT. YMAG(I)) GO TO 38
    PK(3)=PK(2)
    PK(2)=YMAG(I)
    YFRQ(3, J)=YFRQ(2, J)
    YFRQ(2, J)=OMEG(I)
    GO TO 40
C
38  IF (PK(3) .GT. YMAG(I)) GO TO 40
    PK(3)=YMAG(I)
    YFRQ(3, J)=OMEG(I)
40  CONTINUE
C
DO 45 K=1,3
    XFRQ(K, J)=XFRQ(K, J)/P
    YFRQ(K, J)=YFRQ(K, J)/P
45  CONTINUE
C
    RETURN
    END
C
C
C
SUBROUTINE CYCLE
C

```

C THIS SUBROUTINE CALCULATES THE NUMBER OF CYCLES
C TO FAILURE FOR EACH CONVOLUTION.

C
COMMON/BLOK1/ PI,DELO,PIDEN,ALO,TE,EM,UC,UCT,N
COMMON/BLOK5/ A1,E,BOTX2,BOTY2
COMMON/BLOK6/ SAMP
COMMON/BLOK9/ CFAIL
DIMENSION CFAIL(5),SAMP(5)
REAL NF

C
B=-0.1
C=-0.7
D=(12.*150000.)/E

C
DO 30 J=1,N
NF=10.
NUM=1
10 FNF=D*((2.*NF)**B)+((2.*NF)**C)-SAMP(J)/2.
FNF1=2.*B*D*((2.*NF)**(B-1.))+2.*C*((2.*NF)**(C-1.))
DELNF=FNF/FNF1
IF (ABS(DELNF) .LE. 0.5) GO TO 20
NF=NF-DELNF
NUM=NUM+1
IF (NUM .GT. 50000) GO TO 40
GO TO 10
20 CFAIL(J)=NF
30 CONTINUE
GO TO 45
40 PRINT*, ' CONVERGENCE PROBLEM IN CYCLE.'
45 RETURN
END

C
C
C
SUBROUTINE DAMAGE

C
C THIS SUBROUTINE COMPUTES THE DAMAGE DONE TO
C EACH CONVOLUTION DURING SAMPLING PERIOD WHICH
C INDICATES THE CONVOLUTION MOST LIKELY TO
C FAIL FIRST.

C
COMMON/BLOK1/ PI,DELO,PIDEN,ALO,TE,EM,UC,UCT,N
COMMON/BLOK8/ XFRQ,YFRQ
COMMON/BLOK9/ CFAIL
COMMON/BLOK10/ NFAIL,FMAX,FMIN
DIMENSION XFRQ(3,5),YFRQ(3,5),CFAIL(5),D(5)

C
DO 20 J=1,N
SUM=0.0
DO 10 K=1,3
TERM=XFRQ(K,J)+YFRQ(K,J)
SUM=SUM+TERM
10 CONTINUE
SUM=0.02048*SUM
D(J)=SUM/CFAIL(J)
20 CONTINUE

C
DTEST=0.0
DO 30 J=1,N
IF (D(J) .LT. DTEST) GO TO 30

```

DTEST=D(J)
NFAIL=J
30 CONTINUE
C
XFMAX=0.0
XFMIN=1000000.0
YFMAX=0.0
YFMIN=1000000.0
DO 40 K=1,3
IF (XFRQ(K,NFAIL) .EQ. 0.0) GO TO 40
XFMAX=AMAX1(XFRQ(K,NFAIL),XFMAX)
XFMIN=AMIN1(XFRQ(K,NFAIL),XFMIN)
40 CONTINUE
DO 50 K=1,3
IF (YFRQ(K,NFAIL) .EQ. 0.0) GO TO 50
YFMAX=AMAX1(YFRQ(K,NFAIL),YFMAX)
YFMIN=AMIN1(YFRQ(K,NFAIL),YFMIN)
50 CONTINUE
C
FMAX=AMAX1(XFMAX,YFMAX)
FMIN=AMIN1(XFMIN,YFMIN)
C
RETURN
END
C
C
C
SUBROUTINE RESULT
C
C THIS SUBROUTINE PRODUCES THE DESIRED OUTPUT.
C
COMMON/BLOK1/ PI,DELO,PIDEN,ALO,TE,EM,UC,UCT,N
COMMON/BLOK9/ CFAIL
COMMON/BLOK10/ NFAIL,FMAX,FMIN
DIMENSION CFAIL(5)
C
TMAX=CFAIL(NFAIL)/FMIN
TMIN=CFAIL(NFAIL)/FMAX
C
PRINT*, '** NUMBER OF CYCLES TO FAILURE:'
PRINT*, '** ',CFAIL(NFAIL)
PRINT*, '** '
PRINT*, '** MINIMUM TIME TO FAILURE:'
PRINT*, '** ',TMIN,' SEC.'
PRINT*, '** '
PRINT*, '** MAXIMUM TIME TO FAILURE:'
PRINT*, '** ',TMAX,' SEC.'
C
RETURN
END

```

APPENDIX III

SAMPLE DATA FROM PROGRAM

The following charts show the cycles to failure, (N_f), taken from several test runs of the computer program. In each case the fluid flowing through the bellows is taken to be water with a density of 0.036 lbm/in^3 . N_c is the number of convolutes and U_c is the flow velocity in ft/s.

Bellows 1

Convolute pitch = 0.34 in.

Convolute height = 0.492 in.

Ply thickness = 0.015 in.

Number of plies = 1

Bellows inside diameter = 4.55 in.

Elastic modulus = 29×10^6 psi

Material density = 0.286 lbm/in^3

Cycles to Failure

$U_c \backslash N_c$	2	3	4	5
10	1.9×10^7	1.3×10^9	2.1×10^9	5.9×10^9
20	1.6×10^6	8.0×10^6	4.5×10^5	2.0×10^5
30	4.4×10^6	1.4×10^8	1.7×10^6	4.1×10^5
40	4.7×10^7	2.9×10^9	3.5×10^7	4.2×10^6
50	8.8×10^6	6.0×10^7	3.6×10^6	8.6×10^6
60	2.4×10^5	1.2×10^6	6.2×10^5	2.5×10^5

Bellows 2

Convolute pitch = 0.3 in.

Convolute height = 0.395 in.

Ply thickness = 0.01 in.

Number of plies = 2

Bellows inside diameter = 4.47 in.

Elastic modulus = 29×10^6 psi

Material density = 0.286 lbm/in^3

Cycles to Failure

$U_c \backslash N_c$	2	3	4	5
10	3.3×10^8	4.0×10^{10}	8.9×10^{10}	2.3×10^{10}
20	3.3×10^7	3.4×10^8	5.5×10^7	8.3×10^6
30	9.7×10^7	2.3×10^9	6.1×10^7	7.8×10^6
40	1.8×10^8	5.0×10^{10}	1.4×10^9	2.2×10^8
50	2.8×10^7	8.9×10^8	1.8×10^8	3.3×10^7
60	4.0×10^6	1.6×10^7	2.1×10^7	8.4×10^6

MSFC TEST BELLOWS

BELLOWS NO.	V _F (FPS)	TIME TO FAILURE (SEC)	CYCLES TO FAILURE (X10 ⁶)	MATERIAL	ACTUAL STRESS (PSI)	VARIATION
5002-1	62	148-158	.17-.18	321	29,800	ELBOW
5002-2	72	525-535	.70-.71	321	28,300	ELBOW
5002-3	48	313-333	.34-.36	321	29,000	ELBOW
5002-4	56	2255-2309	2.5-2.6	321	27,800	ELBOW
5002-5	70	10460-10585	16.0-16.1	321	26,500	ELBOW
5002-6	70	730-736	.95-.96	321	28,100	ELBOW
5005-1	33.2	1841-1863	.78-.79	321	28,200	
5005-2	65.2	75-100	----	321	33,000	ELBOW
5006-10	77.7	1500-1530	1.7	321	27,900	
5009-1	40.5	2728-2743	1.8	321	27,900	
5011-1	49.4	3107-3133	1.9	321	27,600	
5013-2	50	2007-2027	1.3	321	28,000	
5013-3	45	749-760	.47-.48	321	28,800	
5028-1	65.8	787	----	21-6-9	33,000	ELBOW
5028-2	66.6	150	.16	21-6-9	37,000	ELBOW
5034-1	82.5	1672	2.3	21-6-9	31,200	λ
5034-2	84	1427-1467	1.9-2.0	21-6-9	31,200	
5034-3	84.2	3391-3402	5.0	21-6-9	31,000	λ
5034-4	84.4	3683	5.3	21-6-9	31,000	λ
5034-5	65.5	353-373	.37-.39	21-6-9	34,000	λ
5034-6	85.5	226-256	.28-.32	21-6-9	34,200	λ
5034-7	85	2199	2.9	21-6-9	31,000	λ
5034-8	85.8	560-590	.74-.78	21-6-9	31,900	
5034-10	70.9	3580-3760	3.9-4.1	21-6-9	31,000	
5034-13	79.5	1375-1495	1.6-1.8	21-6-9	31,200	
5034-15	69	4180	4.5	21-6-9	31,000	
AG#1	57.8	1604-1634	1.7	21-6-9	31,400	
AG#2	74.8	20099-20124	----	21-6-9	----	
AG#3	80.5	11248-11278	----	21-6-9	----	
5035-1	113	1976-1996	4.4-4.5	21-6-9	31,000	
5035-2	110	437-477	.98-1.1	21-6-9	31,800	
5035-3	94	7916-8036	16.3-16.6	21-6-9	31,000	λ

FROM REFERENCE 2.